NASA TECHNICAL MEMORANDUM

NASA TM X- 72639

NASA TM X-72639

(NASA-TM-X-72639) NOISE REDUCTION STUDIES FOR THE OV-1 AIRPLANE (NASA) 68 p HC $4.25 CSCL 01C

N75-18232

Unclas
G3/07 12414

NOISE REDUCTION STUDIES FOR THE OV-1 AIRPLANE

By D. A. Hilton, A. B. Connor, W. L. Copeland, and

A. C. Dibble, Jr.

April 1975

NATIONAL AERONAUTICS AND SPACE ADMINISTRATION

LANGLEY RESEARCH CENTER, HAMPTON, VIRGINIA 23665

1. Report No.	2. Government Accession No.	3. Recipient's Catalog No.
TM X-72639		

4. Title and Subtitle	5. Report Date
Noise Reduction Studies for the OV-1 Aircraft	April 1975
	6. Performing Organization Code 26.200

7. Author(s)	8. Performing Organization Report No.
D. A. Hilton, A. B. Connor, W. L. Copeland, and A. C. Dibble, Jr.	

9. Performing Organization Name and Address	10. Work Unit No.
NASA Langley Research Center Hampton, Virginia 23665	505-03-12-05
	11. Contract or Grant No.

12. Sponsoring Agency Name and Address	13. Type of Report and Period Covered
National Aeronautics and Space Administration Washington, DC 20546	NASA Technical Memorandum
	14. Sponsoring Agency Code

15. Supplementary Notes
This information was published in an informal document in 1967. No attempt is made to update this material to reflect the current state of the art.

16. Abstract

A study has been conducted to define possible modifications to the OV-1 aircraft to reduce its aural detection distance. This effort involved documenting the noise characteristics of the airplane, devising modifications to reduce the noise, estimating the reduction in detection distance, and evaluating aircraft performance as a result of these modifications.

It was found that the main noise source on this aircraft is the propeller and hence modifications only to the propeller and the propeller drive system are proposed. Modifications involving only the propeller are noted to involve no increase in weight but they result in only a modest decrease in aural detection distance. In order to obtain substantial decreases in aural detection distance, modifications involving changes both to the propeller and the engine-propeller gearing are required.

17. Key Words (Suggested by Author(s)) (STAR category underlined)	18. Distribution Statement
Acoustics, aircraft noise, propellers, aural detection, and noise reduction	Unclassified - Unlimited

19. Security Classif. (of this report)	20. Security Classif. (of this page)	21. No. of Pages	22. Price*
Unclassified	Unclassified	68	$4.25

*Available from { The National Technical Information Service, Springfield, Virginia 22161
STIF/NASA Scientific and Technical Information Facility, P.O. Box 33, College Park, MD 20740

NOISE REDUCTION STUDIES FOR THE OV-1 AIRPLANE

By D. A. Hilton, A. B. Connor, W. L. Copeland, and
A. C. Dibble, Jr.

SUMMARY

A study has been conducted to define possible modifications to the OV-1 aircraft to reduce its aural detection distance. This effort involved documenting the noise characteristics of the airplane, devising modifications to reduce the noise, estimating the reduction in detection distance, and evaluating aircraft performance as a result of these modifications.

It was found that the main noise source on this aircraft is the propeller and hence modifications only to the propeller and the propeller drive system are proposed. Modifications involving only the propeller are noted to involve no increase in weight but they result in only a modest decrease in aural detection distance. In order to obtain substantial decreases in aural detection distance, modifications involving changes both to the propeller and the engine-propeller gearing are required.

INTRODUCTION

NASA in response to a Department of Defense request has undertaken a study of the noise reduction potential of the OV-1 airplane in terms of the aural detection distance. This effort specifically involves: (1) documenting

the noise characteristics of the basic airplane, (2) evaluating possible modifications and their associated noise reductions, (3) estimating the effect of some selected modifications on the aural detection distance of the aircraft, and (4) estimating the effects of such noise reduction modifications on the performance and stability of the aircraft. This paper documents the NASA efforts in accomplishing the above objectives.

SYMBOLS

A	propeller disk area
B	number of propeller blades
C_D	drag coefficient, $\frac{\text{drag}}{1/2\rho V^2 S}$
C_L	lift coefficient, $\frac{\text{lift}}{1/2\rho V^2 S}$
C_P	power coefficient, $\frac{550\ \text{SHP}}{\rho\, n^3\, D^5}$
C_T	thrust coefficient, $\frac{\text{thrust}}{\rho\, n^2\, D^4}$
D	propeller diameter, ft
M_t	propeller rotational tip Mach number
N	revolutions per minute
R	propeller tip radius, ft
S	wing area
T	thrust
V	velocity, true airspeed
X	slant range distance from airplane to observer
dB	decibels, re 0.0002 dynes/cm^2

f	frequency, cps
m	order of harmonic of propeller
n	revolutions per second
q_o	free-stream dynamic pressure
q_t	dynamic pressure at the tail
Ψ	azimuth angle measured from the thrust axis of propeller (0° is in front)
η	propeller efficiency, $\frac{C_T}{Cp} \times \frac{V}{nD}$
σ	propeller blade element solidity
ρ	mass density of air
cps	cycles per second
V/nD	propeller advance ratio parameter
MAC	mean aerodynamic chord
MRP	military rated power
NRP	normal rated power
SHP	shaft horsepower
TAS	true airspeed
THP	thrust horsepower
T.O.	take-off

APPARATUS AND METHODS

Test Airplane

The OV-1 airplane which was tested for the studies of this report is a two-place twin-turboprop mid-wing monoplane with a design gross weight of about 14,700 pounds. The free turbine engines are rated at 1,005 hp at

take-off and they are geared to three-bladed 10.0-foot-diameter constant speed propellers. Photographs of the test airplane are shown in figure 1, and a three-view drawing of the airplane with a list of its principal physical features is presented in figure 2. The airplane and the test pilots came from the All Services Evaluation Group, Patuxent River Naval Air Station.

Test Conditions

Noise measurement tests were conducted on September 7, 1966, at the NASA Wallops Island test facility where use was made of the main paved runway surface and the associated flat terrain for locating the instrumentation for both static and flyby tests. The terrain features of the test area are shown in the photograph of figure 3(a) which is a view of the microphone array looking north from the runway center line and figure 3(b) which is a view to the south. Schematic diagrams of the microphone arrays for these tests are included in figure 4. Airplane operating conditions for all noise measurement tests are listed in table I.

Noise Measuring Equipment

The noise measuring instrumentation used for these tests is illustrated by the block diagram of figure 5. The microphones were of a conventional crystal type having a frequency response flat to within ±3 dB over the frequency range of 20 to 12,000 cps. The outputs of all the microphones at each station were recorded on multichannel tape recorders. The entire sound measurement system was calibrated in the field before and after the measurements by means of conventional discrete frequency calibrators supplied by the microphone manufacturers. The data records were played back from the

tape (using the playback system shown schematically in fig. 5) to obtain the sound pressure level time histories and both broad-band and narrow-band spectra.

Aircraft Operation

Static noise surveys.- Static data were taken with the array shown in figure 4 where the microphones were positioned at 30° intervals on 100-foot radii about the propeller hub of the left engine. Only one engine was operated in order to eliminate synchronizing problems and to identify individual noise components from the propeller and other sources. The propeller was operated at five separate speeds as listed under "Static" in table I. Three of the propeller speeds were well below flight operating values, and two were nominally at cruise flight values.

Flyover noise surveys.- In the flyover noise survey with both engines operating at identical power settings the aircraft was flown over a ground track as shown schematically in figure 4. Three power conditions at each of three altitudes were recorded, as listed under flight in table I, where the propeller speeds were 1,200, 1,450, and 1,675 rpm, and the altitudes varied from 50 to 1,030 feet. Geometric altitude and course direction were measured by a GSN/5 radar tracking unit. Position information was relayed to the pilot as an assist and the desired flight path was maintained for about 1 mile prior to and beyond the overhead position.

Atmospheric Conditions

During the time of the tests, observations of surface temperature, humidity, wind velocity, and wind direction were taken in the vicinity of the test site. The temperature ranged from 18.3° C to 26.7° C over a 6-hour

period; the relative humidity changed from 61 to 32 percent, and the wind was from the northwest, variable between 4 and 9 knots over the same period of time.

MEASURED NOISE CHARACTERISTICS OF THE BASIC AIRCRAFT

Static Ground Tests

Results of octave band analyses for the two cruise power static test conditions are listed in table II. This table includes the sound pressure levels in each octave band for six azimuth stations from 360° to 210°. From these data octave band and overall noise level directivity patterns can be determined. It can be seen that the highest overall levels occur in front of the engine and near the propeller plane. The noise levels in front contain mainly high frequency components, whereas those in the propeller plane contain mainly low frequency components. The results of previous studies suggest that the lower frequencies are the more significant in the aural detection problem.

Plots of the octave band spectra for the two engine operating conditions are presented in figure 6. These data are from the 270° microphone position of table II. Both of these spectra are seen to have the highest levels in the second octave band and the octave band levels decrease generally as frequency increases. In this respect the spectra are representative of those for which propeller rotational noise dominates. The increased levels in the highest octave band are believed to be associated with broad-band noise from compressor and turbine components.

Narrow-band analyses are particularly useful for identifying the sources of individual noise components. A sample portion of a narrow-band analysis

record, obtained with the aid of a 3 cps band-width filter is shown in figure 7. The data of the record apply directly to a propeller operating condition of 1,450 rpm and an azimuth angle of 270°. The vertical scale represents noise levels in decibels, whereas the horizontal scale is linear and represents frequency in cycles per second. Only the first 500 cps portion of the record is included for illustration. Several prominent peaks associated with the propeller are noted. Other peaks on the record which may be associated with engine accessories, and so forth, are generally at lower levels than the propeller noise components. Results of narrow band analyses for the 1,200-rpm condition (chosen because of a better potential for noise reduction than the 1,450-rpm condition of fig. 7) are listed in table III for several azimuth locations. All peaks correspond to propeller frequencies with the exception of the one at 345 cps. Narrow-band analyses at the higher frequencies revealed no prominent discrete frequency peaks associated with the compressor and turbine components.

It is obvious that the propeller noise components dominate the noise spectrum of the OV-1 airplane and thus are the important ones with respect to aural detection.

Flyby Tests

Figure 8 contains flyover noise levels for two propeller speed conditions. The data were recorded at the center-line microphone of figure 4 and at slant range distances of 292 and 322 feet for flight runs 2 and 5 (see table I), respectively. In this figure, overall sound pressure levels are plotted as a function of time from an arbitrary reference time. The flight direction of the aircraft is from left to right in the figure. For

both power conditions the noise levels build up to a maximum when the aircraft is essentially overhead. The cyclic nature of the noise level traces results from phasing variations of the two propellers.

Octave band spectra have been obtained for the flight conditions of figure 8 and they are presented in figure 9. These data represent the maximum values in each octave band as the aircraft flies overhead, regardless of when that maximum value occurred. Also shown in the figure are the relatively low ambient noise levels at the times of measurement. It can be seen that the in-flight spectra have somewhat different shapes than were obtained for comparable propeller speeds of the static case. These differences may be accounted for partly by directivity pattern variations and by Doppler effects. The 1,200 propeller rpm data will be used in the determination of detection distance for the basic configuration.

AIRCRAFT MODIFICATIONS ANALYZED

As a result of the analyses of the noise measurements of the basic aircraft in which it was learned that the propeller was the main source of noise, several modifications to the propeller have been evaluated for the purpose of reducing the aural detection distance of the airplane. Low-power cruise flight was the only condition treated for this study and three modifications were selected as having the best potential for reduced aural detection distance. These include increasing the number of propeller blades from 3 to 5 (cases I and II), or to 6 (case III); reducing the propeller diameter (case I); and reducing the propeller speed (cases II and III). The estimated overall noise reduction from 300 feet is 6, 10, and 13 dB, respectively, for cases I, II, and III.

The pertinent parameters describing the propellers and the propeller drive system are listed in table IV. Some of the details of the studies relating to the noise generation, weights, and performance are presented in appendixes A through C.

ESTIMATED NOISE CHARACTERISTICS OF THE MODIFIED AIRCRAFT

A summary of the noise generated as a result of the three modifications to the basic airplane as indicated in table IV are compared to those of the basic airplane in figure 10. This figure is a plot of octave band spectra for a distance of 300 feet for the basic aircraft (measured and calculated) and for the three modifications. The overall sound pressure level for each of the five cases is indicated at the left-hand side of the figure adjacent to the ordinate scale. The sound levels in the lower octave bands of figure 10 represent the results of propeller noise calculations which are presented in Appendix A. The sound levels in the higher octave bands were estimated by adjusting the measured signature by amounts proportional to the estimated propeller vortex noise for the basic airplane and the modifications

It should be noted that some discrepancy exists between the calculations and the measured-in-flight spectra for the basic aircraft. The main components of the noise spectrum in the second, third, and fourth octaves are associated with the propeller rotational noise as calculated in appendix A. It can be seen that the calculated value in the third octave is about 6 dB lower than the measured value during flyover tests whereas agreement is excellent in the other octave bands. The reason for the above discrepancy is not fully

understood, however, it may be due to asymmetry in the noise radiation pattern resulting from nonuniform loading in the propeller disk.

It should be noted that the propellers of this aircraft are not synchronized by design and hence the noise radiation field is time variant. The instantaneous relative position of the propeller blades and the difference in the lengths of propagation paths to the observer are significant factors in determining the level for any particular propeller noise component at the observer location. As a function of time, the noise level of any particular component will vary from a small value to an increase of 6 dB, compared to the level of the corresponding component from a single propeller. Since the maximum noise level is the important feature of the noise exposure in detection, the spectra of figure 10 are based on the maximum noise level, that is, for the fully synchronized condition.

DETERMINATION OF AURAL DETECTION DISTANCE FOR BASIC AND MODIFIED AIRCRAFT

Basic Assumptions Relating to Detection

In addition to the noise source characteristics (see refs. 1 and 2) it is well known that the aural detection of a noise involves such factors as the transmission characteristics of the path over which the noise travels (see refs. 3, 4, 5, 6, and 7) and the acoustic conditions at the observer location (see refs. 4 and 8) as well as the hearing ability of the observer (see ref. 9). Attempts have been made to account for all of the pertinent factors in the above categories for the calculations of detection distance which follow.

Attenuation factors.- The attenuation factors associated with the transmission of noise from the source to the observer are assumed to involve

the well-known inverse distance law, atmospheric absorption due to viscosity and heat conduction, small-scale turbulence, and terrain absorption which is weighted to account for the elevation angle between the source and the observer. For the purposes of this paper these factors are taken into account as determined by the following equation:

$$P.L.\ (f,x) = 20 \log_{10} \frac{x}{A} + \left[K_1 + K_2 + (K_3 - K_1)\, K_4\right] \frac{x}{1000}$$

where propagation loss (P.L.) is computed for each frequency and distance combination and where the first term on the right-hand side of the equation accounts for the spherical spreading of the waves. In this connection x is the distance for which the calculation is being made and A is the reference distance for which measured data are available. The remaining terms which represent propagation losses and which are given in coefficient form are defined as follows:

K_1 represents the atmospheric absorption due to viscosity and heat conduction and is expressed in dB per 1,000 feet. The values of K_1 vary as a function of frequency and for the purposes of this paper are those of the following table. For frequencies up to 500 cps data are taken from reference 3 and for the higher frequencies from reference 6.

Octave band no.	Center freq.	dB loss per 1000 ft
1	31.5	—
2	63	0.1
3	125	.2
4	250	.4
5	500	.7
6	1000	1.4
7	2000	3.5
8	4000	7
9	8000	14.5

K_2 is the attenuation in the atmosphere due to small-scale turbulence. A value of 1.3 dB per 1,000 feet is assumed independent of frequency for the frequency range above 250 cycles (see ref. 7).

K_3 also is expressed in dB per 1,000 feet and includes both atmospheric absorption and terrain absorption. The values used are those of reference 4 which are listed for widely varying conditions of vegetation and ground cover. The data of reference 4 have been reproduced in a more convenient form in reference 5. Calculations included herein make use of the data of reference 5 particularly curve (b) of figure 1 which represents the condition of thick grass cover (18 inches high) and the upperbound of curve 3 of figure 2 which represents conditions of leafy jungle with approximately 100 feet "see through" visibility. K_4 is a weighting factor to account for the angle, measured from the ground plane, between the noise source and the observer. The values of K_4 assumed for the present calculations were taken from figure 3 of reference 5 and are seen to vary from zero for angles greater than 7° to 1.0 for an angle of 0°.

Ambient noise level conditions and human hearing.- The detectability of a noise is also a function of the ambient masking noise conditions at the listening station and the hearing abilities of the listener. Since they are somewhat related, they will be discussed together.

The ambient noise level conditions assumed for these studies were based on data from references 4 and 8 which were obtained in jungle environments. It was indicated in reference 3 that a noise made up of discrete tone components is detectable if it is within 9 dB of the background noise (random in nature) in any particular octave band. Thus, the corresponding measured

spectra of references 4 and 8 have been reduced by 9 dB to account for the above difference in the masked and the masking spectra.

The resulting octave band spectra have been further adjusted to account for critical band width of the human ear, according to the following equation, to give masking level values for each band.

$$\text{Masking level, dB} = \text{octave band level, dB} - 10 \log_{10} \left[\frac{\Delta f_{octave}}{\Delta f_{critical}} \right]$$

where the Δf_{octave} and $\Delta f_{critical}$ values corresponding to standard octave band center frequencies are given in the following table:

Octave band center freq., cps	31.5	63	125	250	500	1000	2000	4000	8000
Δf_{octave}, cps	22	44	88	177	354	707	1414	2828	5656
$\Delta f_{critical}$, cps	--	--	50	50	50	66	100	220	500
$10 \log_{10} \frac{\Delta f_{octave}}{\Delta f_{critical}}$	--	--	2.5	5.5	8.5	10.7	11.5	11.1	10.5

The values of the last row in the above table have been subtracted from the octave band values to adjust them to the masking level spectra which define the boundaries of the jungle noise criteria detection region of figures 13 through 16.

Likewise a threshold of hearing curve (taken from ref. 3) is made use of since it represents the levels of pure tone noise that are just detectable on the average by healthy young adults. The implication here is that noises having levels lower than those of the threshold of hearing curve at corresponding frequencies will not be detectable. Thus the threshold of hearing curve is the determining factor of detection at the lower frequencies.

No attempt is made to account for possible binaural effects in the studies of the present paper.

Estimation Methods

Reference detection distances for each aircraft configuration for flight altitudes of 1,000 and 3,000 feet and for ground cover conditions representative of both 18-inch grass and 100-foot see-through leafy jungle, have been determined with the aid of figure 11 and the basic noise signature of figure 10. In this figure the octave band noise levels at various distances have been estimated by taking into account the appropriate atmospheric and terrain losses. Also shown in the figure is a threshold of hearing curve and a band labeled "jungle noise detection criteria." The lower boundary of this area represents masking levels in a relatively quiet jungle location in the Canal Zone (ref. 4). The upper boundary on the other hand represents a relatively more noise masking level condition in Thailand (ref. 8). These data have been compared with and found to be generally compatible with results of recent, but unpublished, jungle noise surveys taken at Fort Clayt in the Canal Zone. In the determination of the maximum distance at which the aircraft can be detected aurally, it was assumed that such detection was possible at distances at which the level of aircraft noise in any octave band equaled or exceeded either the masking level curve or the threshold of hearing curve, whichever was more appropriate. The results of such estimates are included in table V for each aircraft configuration and the two altitude and ground cover conditions.

Effects of Aircraft Operating and Ground Observer Conditions

In general, detection distances are shorter for lower aircraft altitudes, as was found in reference 3. Another general conclusion is that the more dense ground cover condition results in detection distances either equal to or smaller than those of the less dense ground cover condition, as previously determined in reference 10.

THE EFFECTS OF AIRCRAFT CONFIGURATION MODIFICATIONS

The aircraft configurations of table V have progressively decreasing values of overall noise level and the associated detection distances decrease in the same manner reading from left to right in the table.

Modification I involves no change in the gearing but does involve an increase in the number of propeller blades from 3 to 5 and a decrease in propeller diameter from 10 feet to 9 feet. It is indicated in table V that this modification will result in modest reductions of the aural detection distances from 22,000 to 17,000 feet and from 38,000 to 23,000 feet for altitudes of 1,000 and 3,000 feet, respectively. It should be noted that no increase in weight is indicated for such a modification.

More ambitious changes to the propeller and drive system are involved in modifications II and III, for which the detection distances are approximately 8,700 and 5,000 feet, respectively. Both modifications utilize 10-foot-diameter propellers. Modification II requires a change in the gear ratio to 0.75 and an increase in the number of blades from 3 to 5 whereas modification III requires a further change in the gear ratio to 0.7 and an increase in the number of blades from 3 to 6. Increases in weights of about

130 pounds and 82 pounds, respectively, are indicated from the analysis of appendix B. The weight increases resulting from these modifications were less than 1 percent and performance penalties were also small. For example, the estimated change in V_{max} is 1.0 knot, V_{stall} changes by only 1.0 knot. There is a slight loss in rate of climb (33 to 91 ft/min), plus a slight increase in take-off distance required (43 to 92 ft.).

CONCLUDING REMARKS

A study has been conducted to define possible modifications to the OV-1 aircraft to reduce its aural detection distance in cruise flight. This effort involved documenting the noise characteristics of the airplane, devising modifications to reduce the noise, and defining the detection distance and aircraft performance as a result of these modifications.

It was found that the main noise source on this aircraft is the propeller and hence modifications only to the propeller and the propeller drive systems are proposed.

1. Modifications involving only the propeller are noted to involve no increase in weight but they result in only a modest decrease in aural detection distance; for example, from 22,000 feet to 17,000 feet at 1,000 feet altitude, and from 38,000 feet to 23,000 feet at 3,000 feet altitude.

2. In order to obtain substantial decrease in aural detection distance, modifications involving changes both to the propeller and the engine propeller gearing are required. In these cases detection distance from altitudes of 1,000 and 3,000 feet and, depending upon terrain, can be reduced by factors ranging from 1/3 to 1/5 to a distance on the order of 1 mile.

3. The effect on aircraft performance resulting from these modifications is shown to be small in most instances, for example, the change in weight is less than 1 percent, and the change in V_{max} and V_{stall} is 1.0 knot. There is a slight loss in rate of climb (33 to 91 ft/min), plus a slight increase in take-off distance required (43 to 92 feet).

REFERENCES

1. Hubbard, Harvey H.; and Maglieri, Domenic J.: An Investigation of Some Phenomena Relating to Aural Detection of Airplanes. NACA TN-4337, September 1958.

2. Vogeley, A. W.: Sound-Level Measurements of a Light Airplane Modified to Reduce Noise Reaching the Ground. NACA Rep. 926, 1949 (Supercedes NACA TN 1647).

3. Loewy, Robert G.: Aural Detection of Helicopters in Tactical Situations. Journal of the American Helicopter Society, vol. 8, no. 4, October 1963.

4. Eyring, Carl F.: Jungle Acoustics. The Journal of the Acoustical Society of America, vol. 18, no. 2, October 1946.

5. Gayne, William J.: Aural Detection of an Aerial Vehicle Operating at Low Altitudes. AIAA paper no. 65-329, July 1965.

6. Anon.: ARP 866, Standard Values of Atmospheric Absorption as a Function of Temperature and Humidity for Use in Evaluating Aircraft Flyover Noise. Society of Automotive Engineers, August 1964.

7. Regier, Arthur A.: Effect of Distance on Airplane Noise. NACA TN 1353, 1947.

8. Anon.: Acoustic and Seismic Research. Semiannual Report No. 3 (ASTIA No. AD 473784) Jansky & Bailey, Research and Engineering Division of Atlantic Research Corporation, October 1965.

9. Fletcher, Harvey: Auditory Patterns. Reviews of Modern Physics, vol. 12, January 1940.

10. Connor, A. B.; Hilton, D. A.; Copeland, W. L.; and Clark, L. R.: Noise Characteristics of the O-1 Airplane and Some Approaches to Noise Reduction. NASA TM X-72638, January 1975.

Table I – List of airplane operating conditions for both the static and flyby noise measurements.

Run no.	Operating condition	Torque psi (a)	RPM (b)	SHP (c)	IAS kts	Altitude above runway, ft.	Lateral displacement from runway, ft
STATIC (LEFT ENGINE ONLY)							
1	ground idle, feathered	9	200	–	–	–	–
2	ground idle, unfeathered	6	500	–	–	–	–
3	flight idle	12	830	–	–	–	–
4	cruise power	40	1200	326	–	–	–
5	cruise power	50	1450	495	–	–	–
FLIGHT (BOTH ENGINES)							
1	cruise power, max. endurance	40	1200	652	132	1030	200E
2					140	250	150E
3					150	60	15W
4	cruise power, max. range	50	1450	990	180	990	0
5					175	320	35W
6					175	50	0
7	climb power	60	1675	1390	205	1000	20E
8					200	300	20W
9					215	50	0

Note: (a) Engine torque indicator gage is calibrated in psi.
(b) Propeller rpm; turbine rpm at normal rated power is 6610.
(c) SHP is calculated from the engine parameters according to the manufacturer's handbook procedure.

Table II - Static noise measurement octave band analysis. Data are from six microphones positioned around the left side of the airplane.

AZIMUTH ANGLE, ψ DEG	OVER-ALL	22 TO 44 CPS	44 TO 88 CPS	88 TO 177 CPS	177 TO 354 CPS	354 TO 707 CPS	707 TO 1414 CPS	1414 TO 2828 CPS	2828 TO 5656 CPS	5656 TO 11,312 CPS
1200 RPM (RUN #4)										
360	78	64	84	85	84	70	70	87	87	73
330	92	58	70	75	82	82	81	78	80	91
300	93	60	75	82	87	87	80	76	73	85
270	93	72	90	83	82	82	80	75	75	81
240	97	75	91	87	89	91	86	81	79	81
210	93	64	76	84	84	87	85	82	77	79
1450 RPM (RUN #5)										
360	106	76	90	97	95	91	91	97	99	100
330	92	76	67	74	78	78	79	79	78	89
300	95	65	86	85	87	87	88	83	77	87
270	103	76	99	98	95	95	92	84	82	86
240	103	76	101	92	93	94	87	87	83	84
210	95	69	79	88	85	87	87	85	83	84

Table III.- Narrow band analyses of the noise from one engine of the OV-1 airplane at a propeller rpm of 1,500.

Freq. CPS	Propeller Harmonic, nB	Sound Pressure Level, dB, at Azimuth Station:—					
		360°	330°	300°	270°	240°	210°
61	3	85	74	--	90	95	78
122	6	83	77	81	84	87	81
183	9	80	83	76	76	86	85
244	12	--	81	79	76	89	82
305	15	82	79	73	78	84	77
345	--	78	65	66	71	72	66
366	18	79	81	77	76	84	75
427	21	79	79	77	76	79	76
488	24	81	73	73	77	76	79
549	27	77	74	75	76	81	75
610	30	84	74	72	77	76	74
671	33	70	75	89	78	76	76
732	36	77	70	67	77	74	69
793	39	75	69	67	75	72	69
854	42	72	68	68	74	73	67
915	45	77	66	70	73	72	66
976	48	70	67	69	70	68	66

NOTE: Data are from the left side engine only; the right side was shut down during these tests.

Table IV.- Summary of Aircraft Modifications

Aircraft Configuration	Propeller				Net Aircraft Weight Increase lbs.	Estimated Overall Noise Level (distance = 300 ft.)
	Mod. gearing / Std. gearing	Dia. ft.	No. of blades	Type*		
Basic OV-1	1.0	10	3	C.P.	----	89 dB (measured) 88 dB (calculated)
Modification I	1.0	9	5	C.P.	-22.2	82 dB
Modification II	0.75	10	5	C.P.	129.2	78 dB
Modification III	0.70	10	6	C.P.	82.2	75 dB

*C.P. - Controllable-pitch propeller

Table V.- Reference aural detection distances in feet for the basic OV-1 Aircraft and for three proposed modifications. Data are for two aircraft altitudes and for two ground cover conditions.

Aircraft Altitude, ft.	Ground Cover	Reference Detection Distance, ft.				
		Aircraft Configuration				
		Basic Measurement	Basic Calculation	Mod. I	Mod. II	Mod. III
1000	grassy	22,000 (b)	20,000 (a)	17,000 (b)	8,500 (c)	5,000 (b)
1000	leafy	15,000 (b)	14,500 (b)	12,000 (b)	8,300 (c)	5,000 (b)
3000	grassy	38,000 (b)	26,000 (b)	23,000 (b)	8,700 (c)	5,000 (b)
3000	leafy	32,000 (b)	26,000 (b)	23,000 (b)	8,700 (c)	5,000 (b)

(a) data from 2nd octave band
(b) data from 3rd octave band
(c) data from 5th octave band

Figure 1.- Photograph of the test airplane.

List of the principal physical dimensions of the OV-1 AF airplane

WING:

Area	330 ft^2
A.R.	5.35
Taper Ratio	.5
Root Chord	10.5 ft
Section	NACA 2412
Dihedral	6.5°
Incidence	1.5°
Flap Area	43.6 ft^2
Aileron Area	22.7 ft^2

HORIZONTAL TAIL:

Area	65 ft^2
A.R.	2.65
Taper Ratio	.5
Root Chord	7.55 ft
Section	NACA 0012
Dihedral	6.5°
Incidence	-1°
Elevator Area	19.0 ft^2

VERTICAL TAILS:

	OUTBOARD	CENTER
Area	21.5 ft^2 each	25.6 ft^2
A.R.	2.06	1.64
Taper Ratio	.46	.54
Root Chord	4.41 ft	5.13 ft
Section	NACA 0012	NACA 0012
Rudder Area	9.5 ft^2 each	8.5 ft^2

WT., EMPTY: 9,360 lb MAX. GROSS WT.: 14,730 lb
TAKE OFF POWER 1005 ESHP
NORMAL RATED POWER 865 ESHP

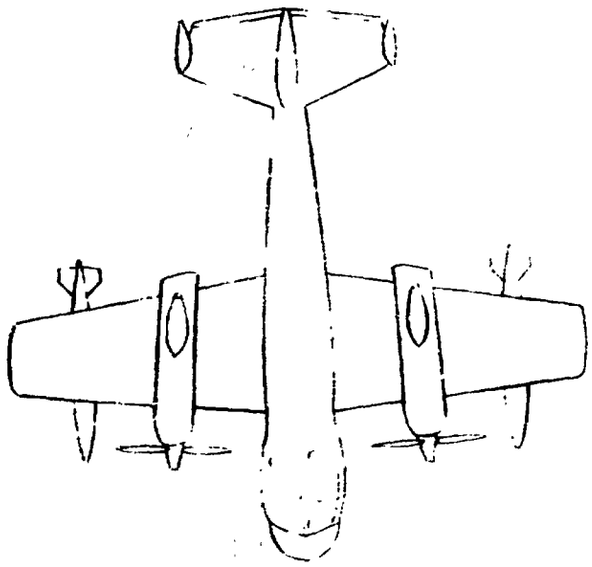

(a) Plan view

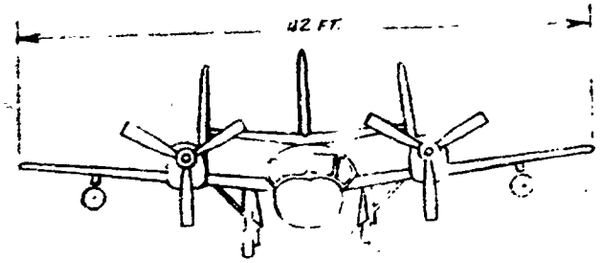

(b) Front view

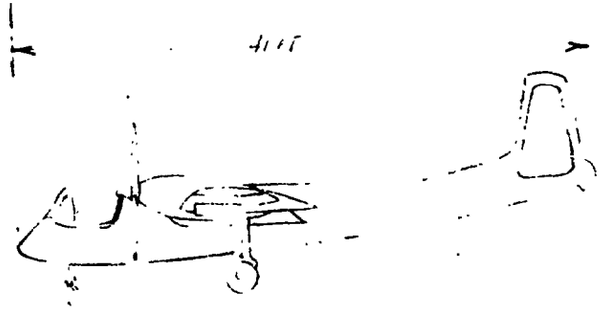

(c) Side view

Figure 2.- Three view sketches of the OV-1 airplane along with a listing of its principal physical features.

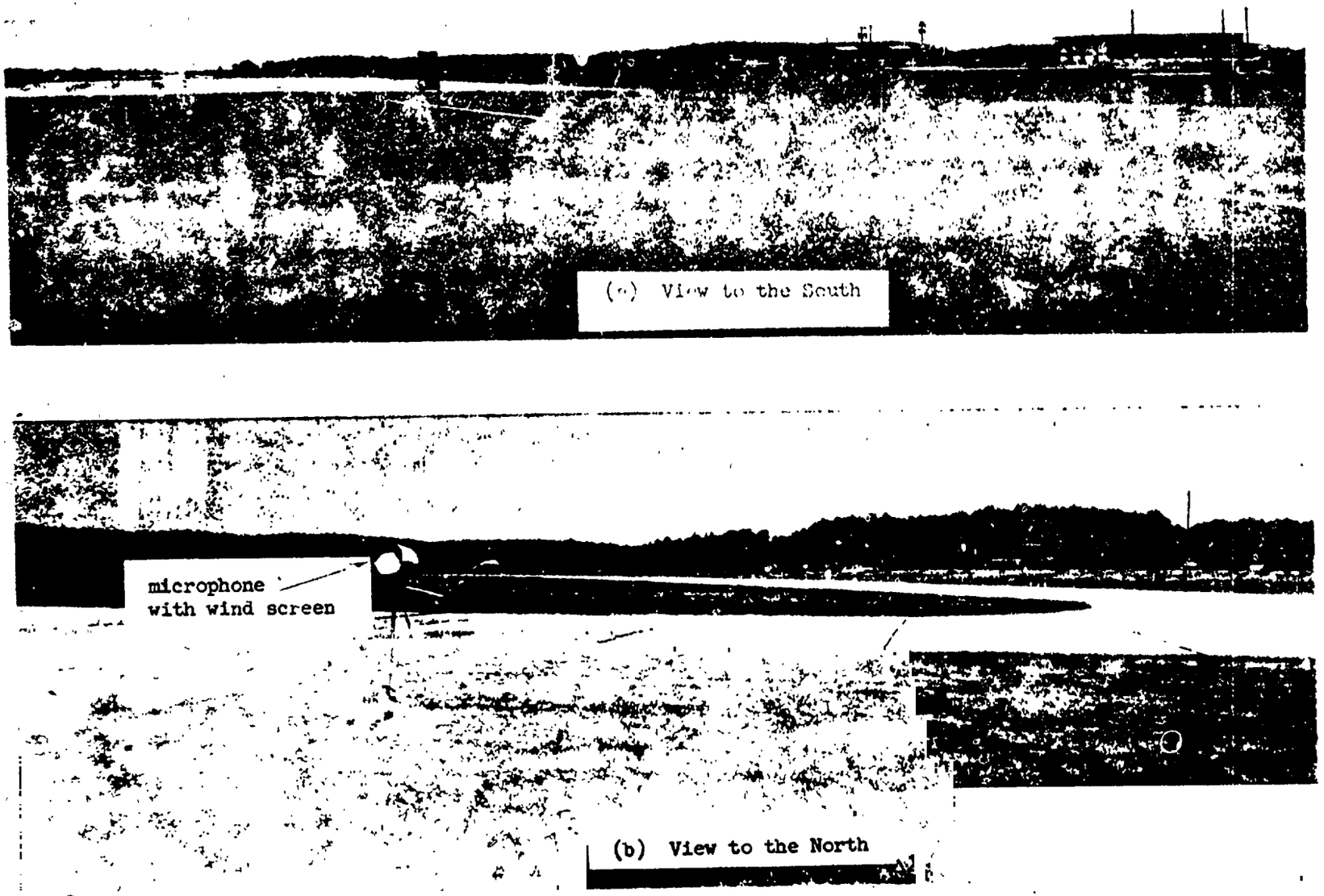

Figure 3.- Photographs of the NASA Wallops Island test area showing the runway and flat terrain.

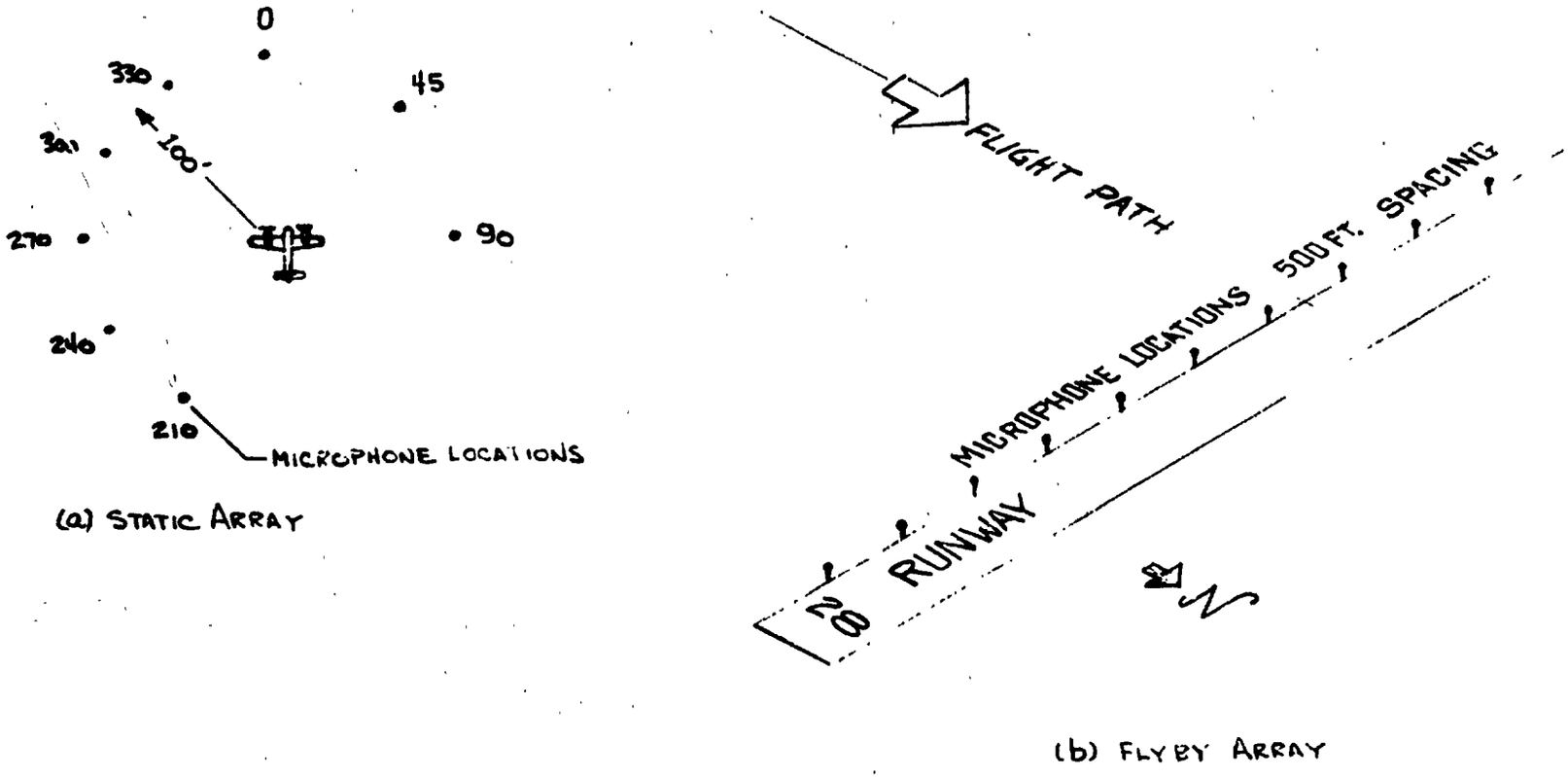

Figure 4.- Diagram of the microphone arrays illustrating the aircraft location for noise measurement during both static and flyby operations.

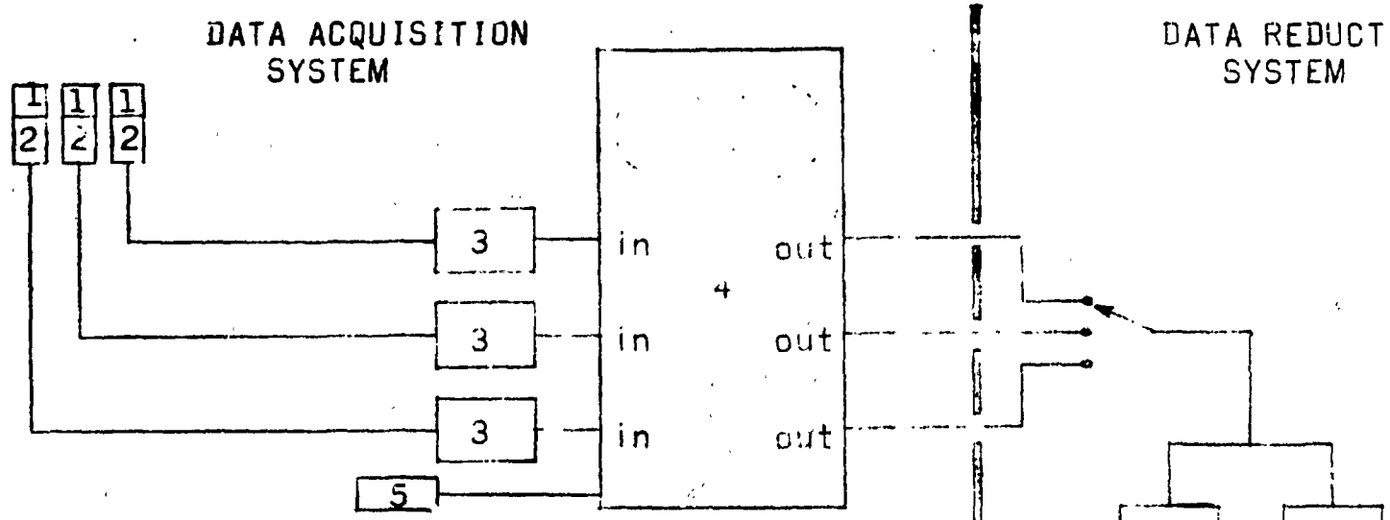

1. G.R. 1560-P5 microphone
2. G.R. 1560-P40 preamplifier
3. G.R. 1551-CS3 sound-level meter
4. Ampex GS-600 tape recorder
5. Altec 633-A "voice" microphone
6. G.R. 1550-AP octave-band analyzer
7. G.R. 1900-A wave analyzer
8. G.R. 1521-B graphic level recorder

Figure 5.- Block diagram showing system layout for noise data acquisition and reduction.

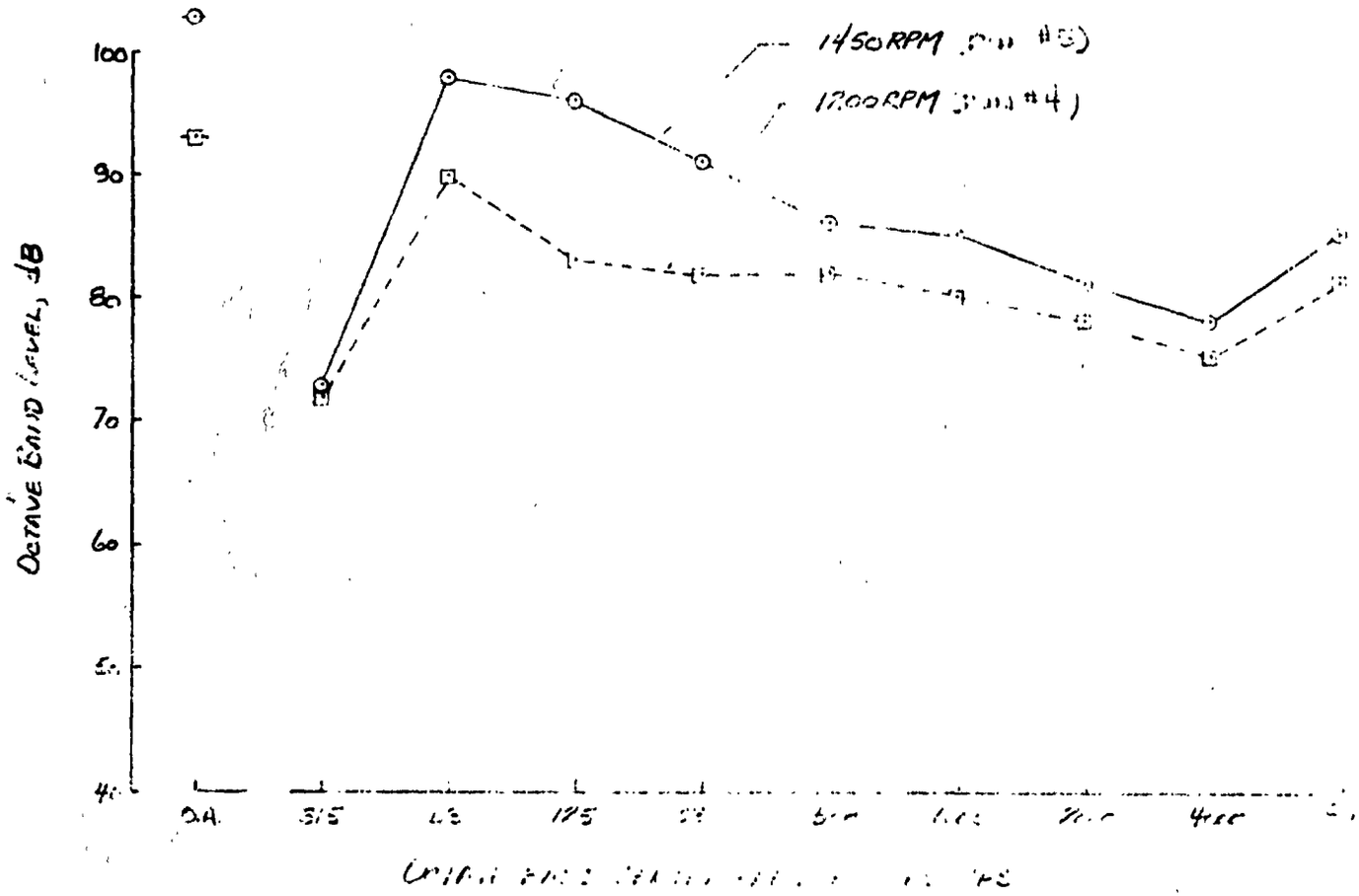

Figure 6.- Octave band noise spectra for the OV-1 airplane during static operation at two engine speeds and at an azimuth angle of 270° (in plane of propeller).

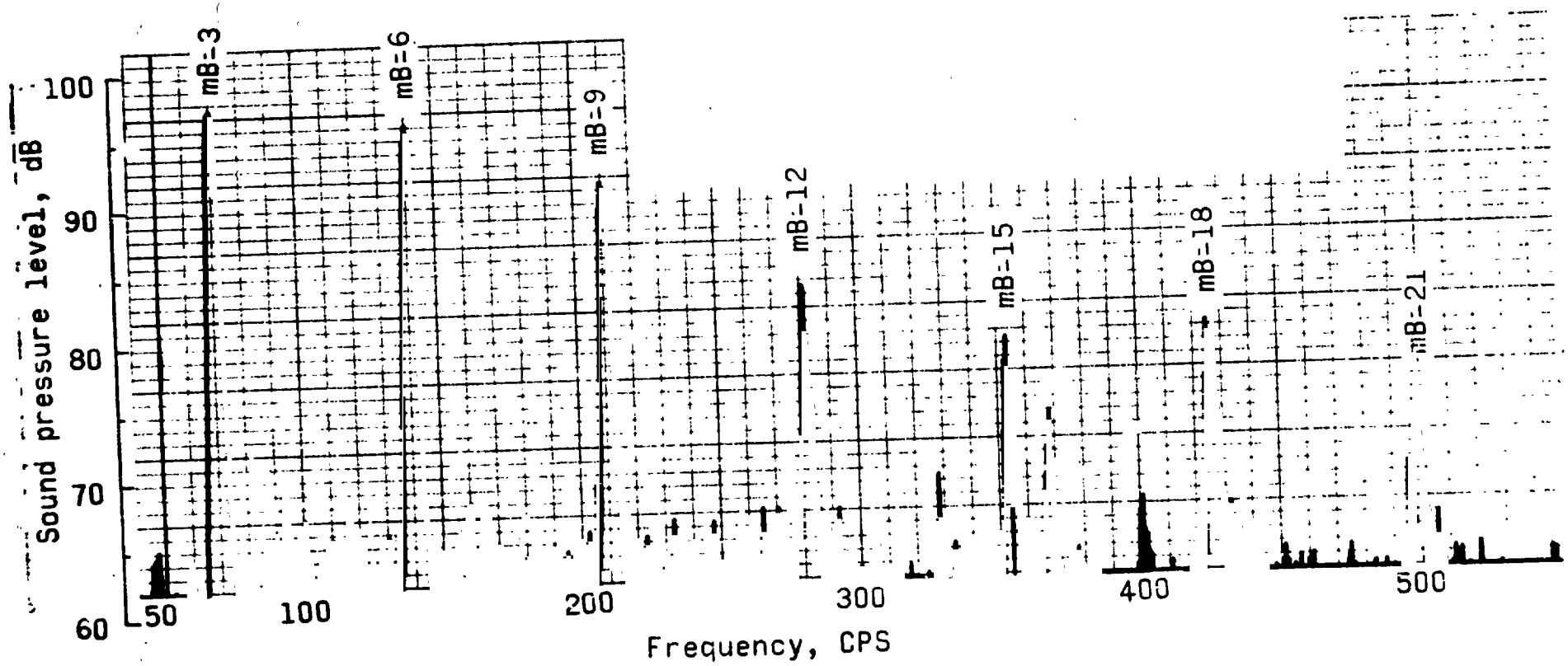

Figure 7.- Sample narrow band (3 cps) record of the noise from one power plant of the OV-1 airplane at a propeller speed of 1,450 rpm and an azimuth angle of 270°.

BY.....DATE.....SUBJECT.....SHEET NO.....OF.....

CHKD. BY.....DATE.....JOB NO.....

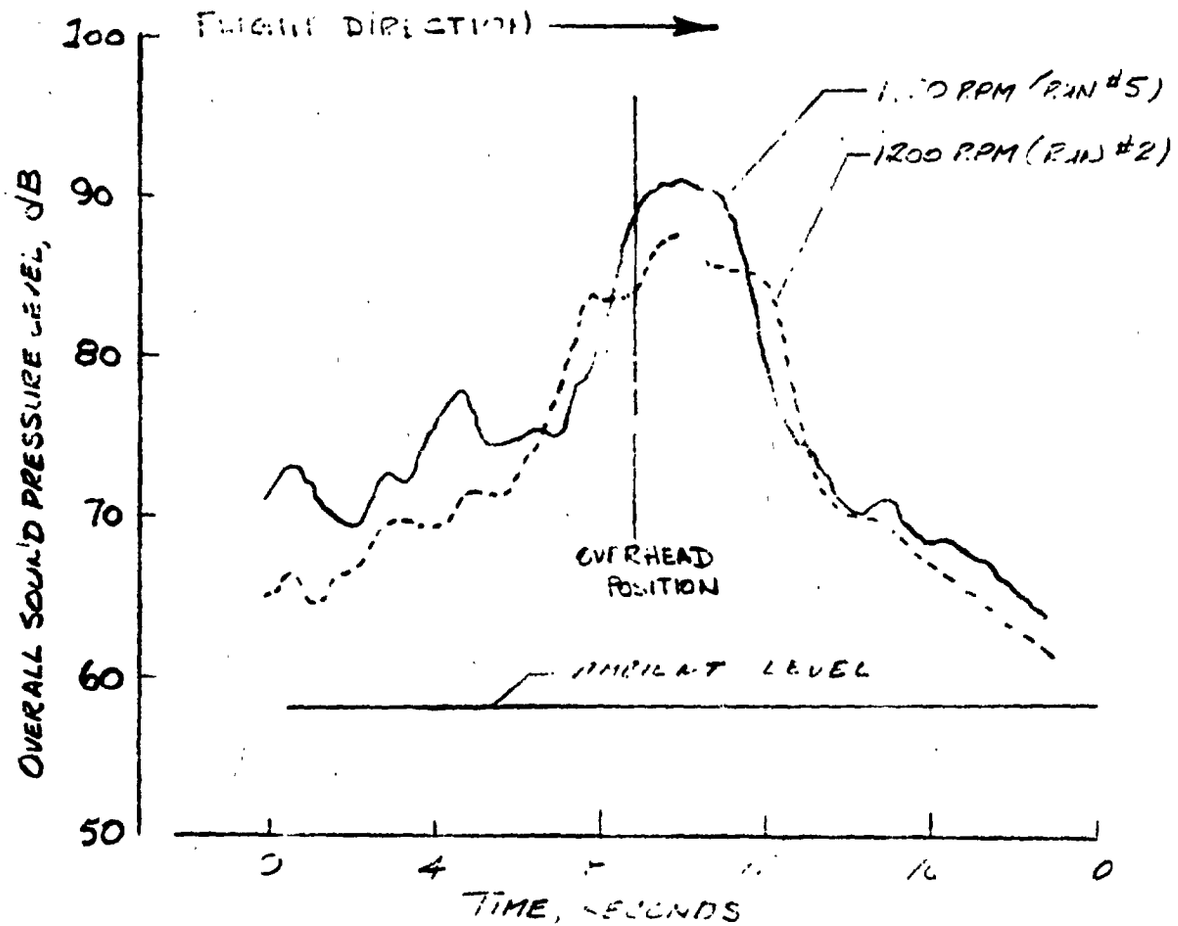

Figure 8.- Overall sound pressure level time histories for OV-1 aircraft during flyby tests for two power conditions.

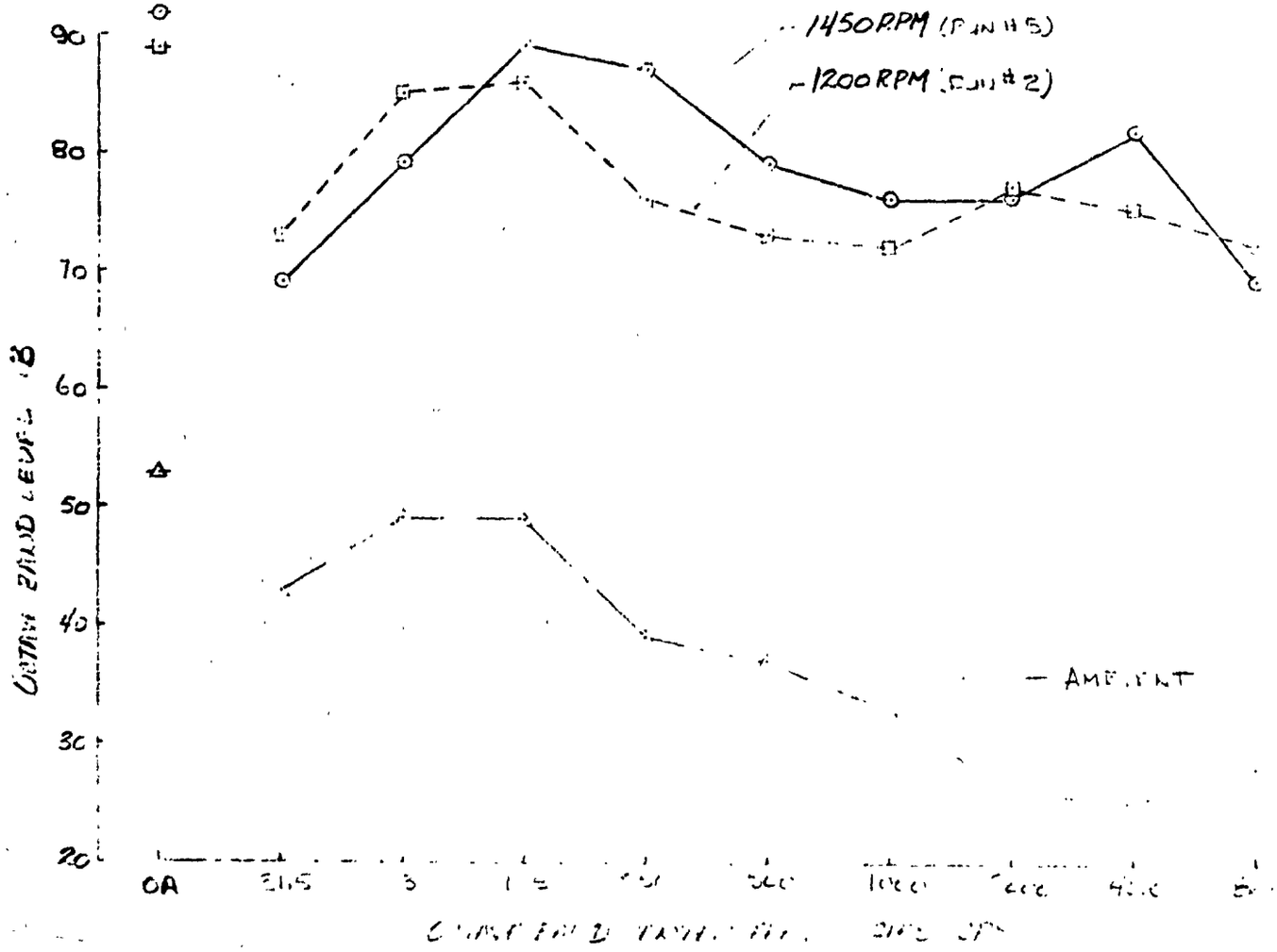

Figure 9.- Octave band spectra of the noise on the ground track from the OV-1 aircraft in flight at two power conditions and at an altitude of 300 feet.
(The levels in each band are the maximum measured regardless of when they occur.)

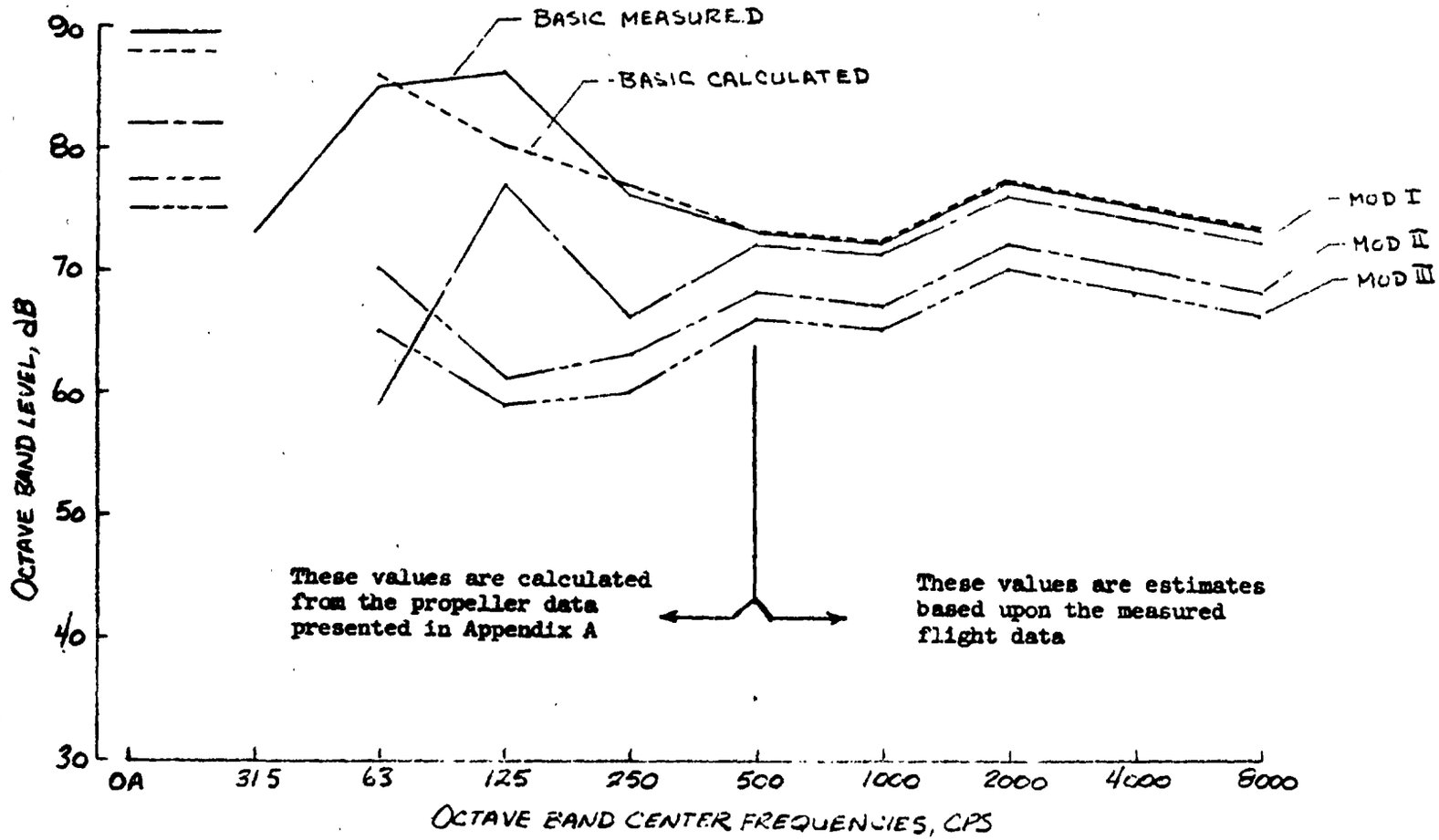

Figure 10.- Estimated octave band spectra for each of the three proposed modifications to the OV-1 aircraft compared to the measured and calculated spectra for the basic aircraft. Data are for a distance of 300 ft.

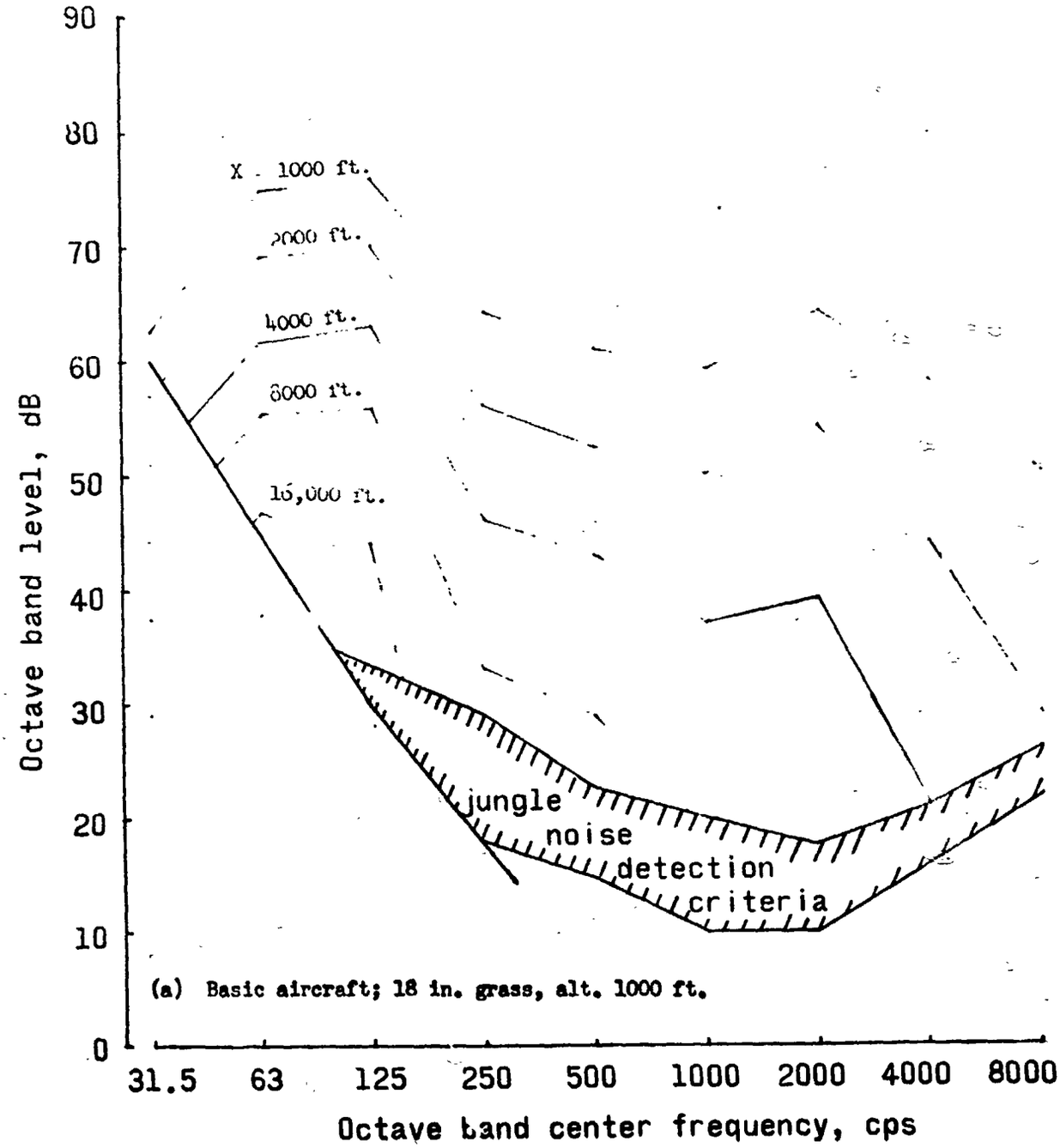

Figure 11.- Estimated noise spectra for basic OV-1 aircraft and for modification III for various slant range distances and altitudes. Data are for grassy (18 in. high) ground cover conditions and for leafy jungle conditions with approximately 100 ft. see-through visibility.

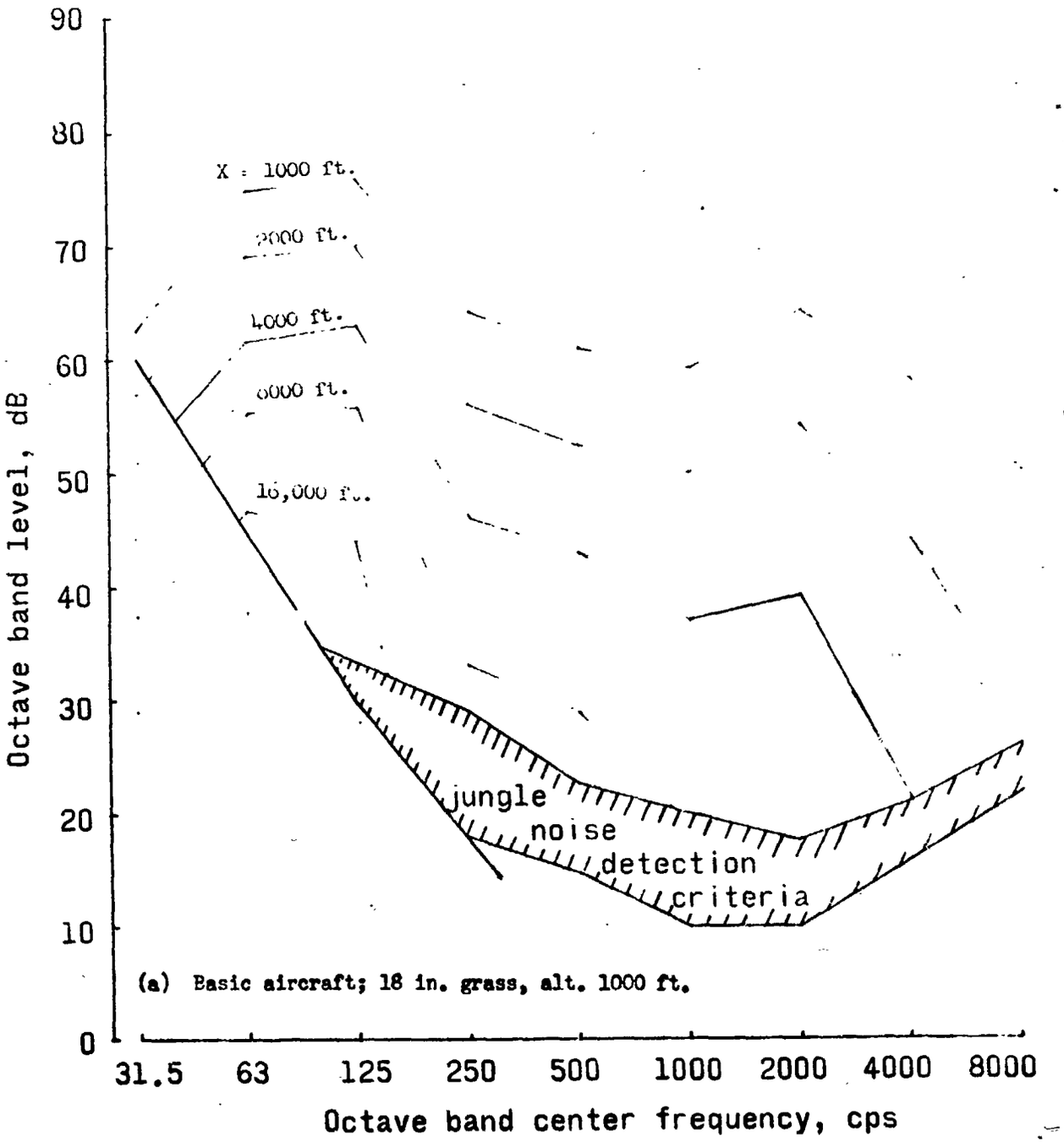

Figure 11.- Estimated noise spectra for basic OV-1 aircraft and for modification III for various slant range distances and altitudes. Data are for grassy (18 in. high) ground cover conditions and for leafy jungle conditions with approximately 100 ft. see-through visibility.

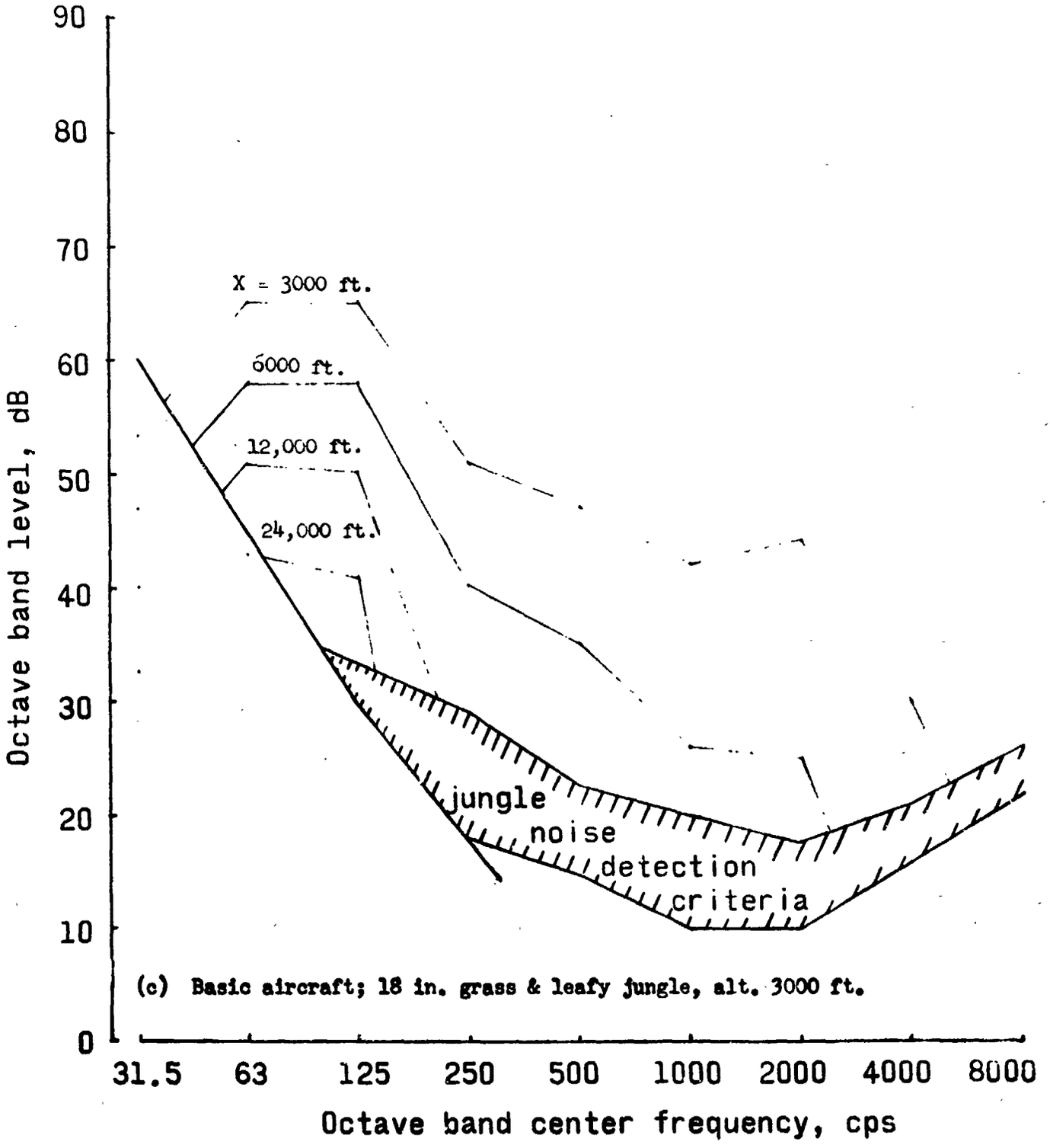

Figure 11.- Continued.

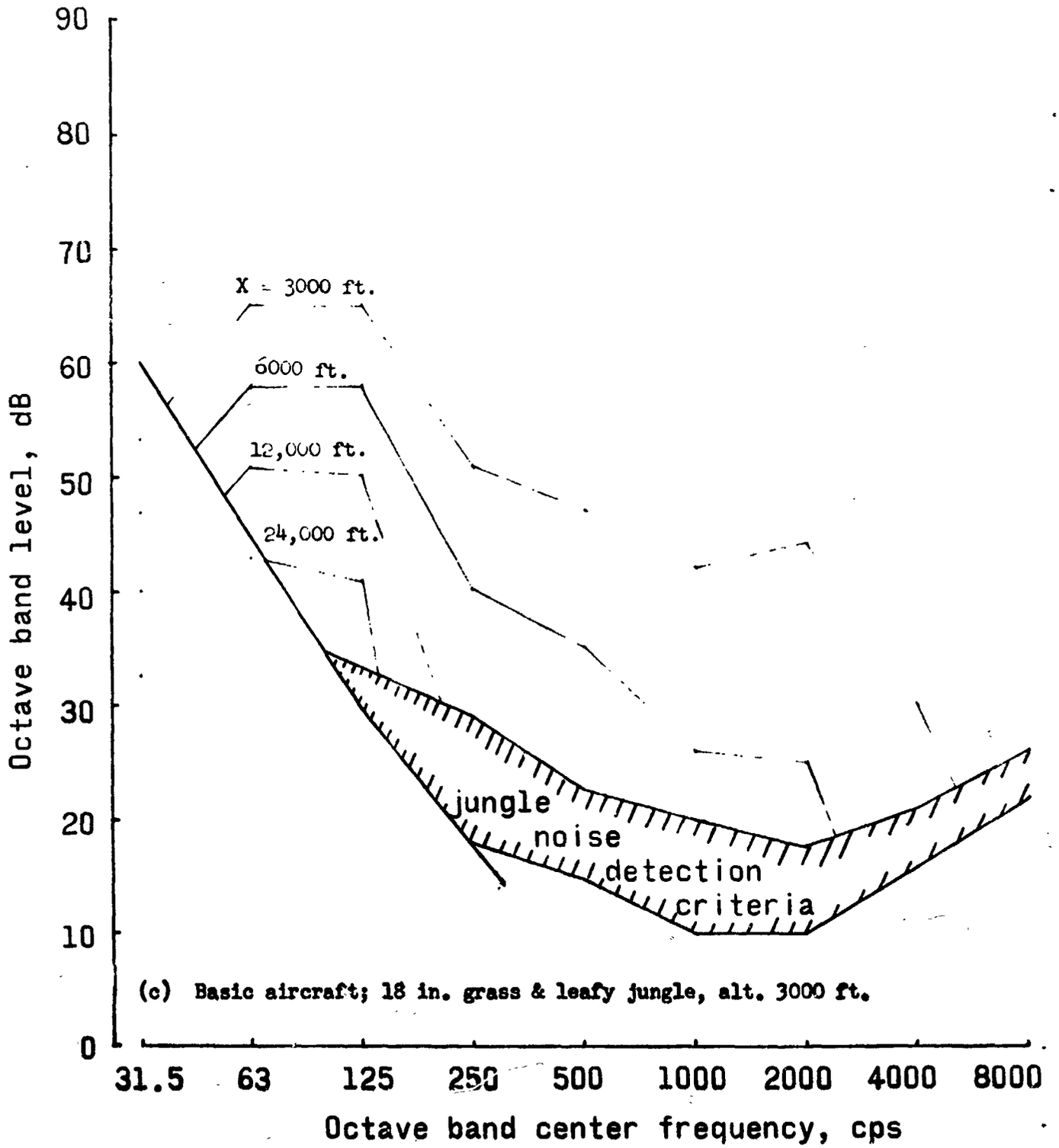

(c) Basic aircraft; 18 in. grass & leafy jungle, alt. 3000 ft.

Figure 11.- Continued.

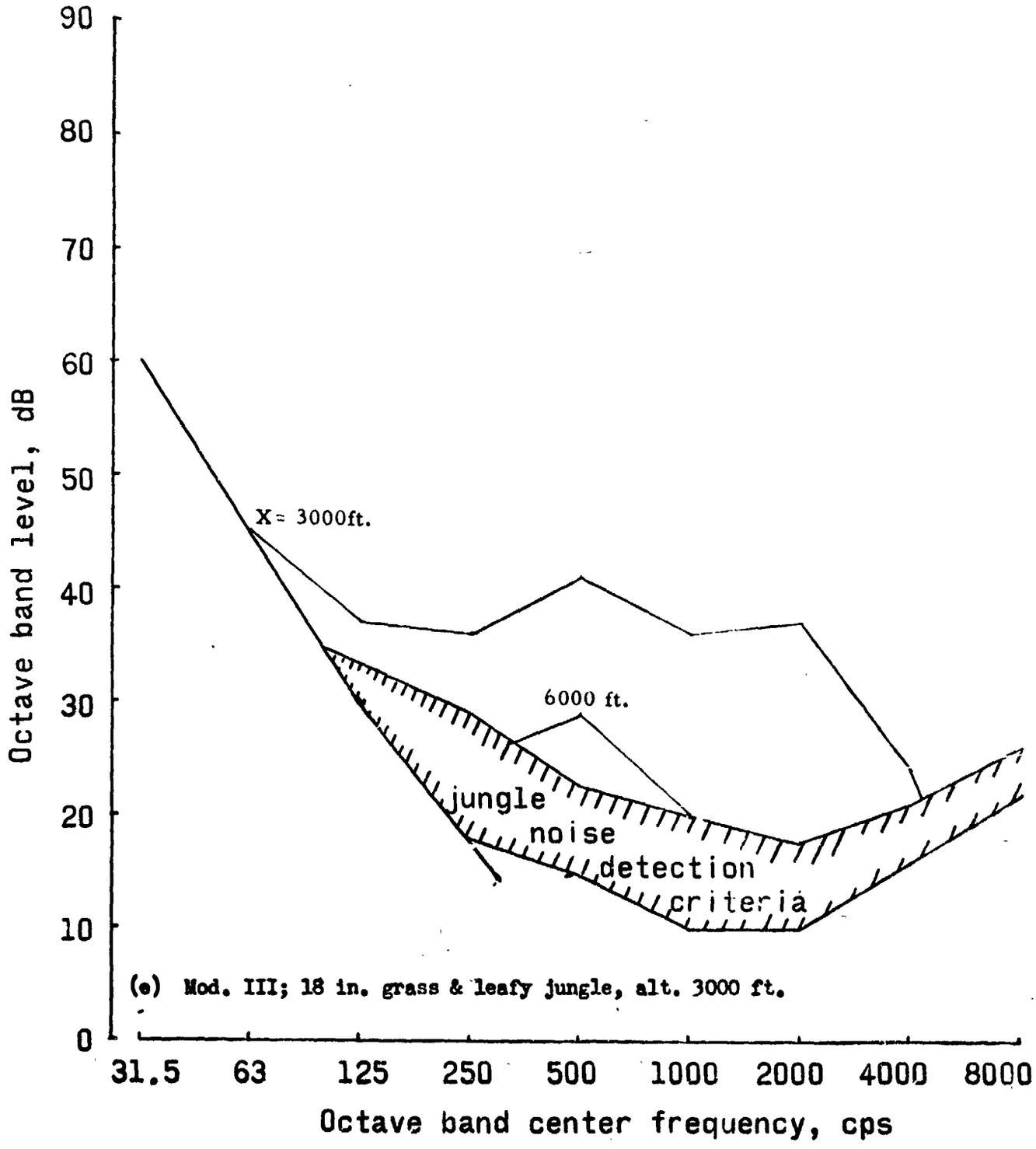

Figure 11.- Concluded

APPENDIX A

PROPELLER NOISE AND PERFORMANCE CONSIDERATIONS

By John L. Crigler

For propeller-driven airplanes, the important parameters to be considered in reducing the propeller noise are the propeller rotational tip speed and the number of blades. References A-1 and A-2 show that for a given design condition the propeller noise can be reduced by a reduction in propeller rotational tip speed or by an increase in blade number, or both. It becomes obvious that the two methods go together; that is, a reduction in rotational tip speed, whether obtained by reduced diameter or reduced rpm, requires an increase in blade number (or wider blades) to absorb the engine power.

This appendix contains a description of the procedure used to estimate the performance of several propellers that could be fitted to the design conditions of the OV-1 airplane, along with estimates of the noise pressures generated by each propeller for minimum power and for level-flight cruise at sea level.

Propeller Sections

The OV-1A airplane is powered by two Lycoming T-53-L-3 turboprop engines. The basic propeller configuration is a 10.0-foot-diameter, three-blade propeller, having a solidity of 0.03815 per blade at the 0.7 radius, designed to absorb 1,015 hp at 1,700 propeller rpm in cruise at 259 knots at sea level. For the present study the maximum propeller diameter has been limited to 10.0 feet, although equally as large or larger reductions in noise pressures may be obtained with increased propeller diameters. Also, increased

take-off performance is possible with larger diameters. Diameters larger than 10 feet were not considered for the OV-1 because of possible fuselage and ground clearance problems.

One alternate propeller design entailed a reduction in diameter to 9.0 feet, with no change in gearing, in order to reduce the rotational tip speed. Because of the decreased diameter, more blade area was required to absorb the power so the blade number was increased to five. Two other designs in which the propeller-to-engine gear ratio was reduced to 75 percent and 70 percent of its present value were selected in order to reduce the rotational tip speed (propeller rotational speeds of 1,275 and 1,190 rpm at the military rated power of 1,015 hp were chosen).

The performance of each of the three alternate propellers has been estimated and these data are compared with the estimated performance of the basic propeller in table A-I. Also listed in table A-I are the number of blades and the solidity at the 0.7 radius (geometrically similar blades assumed) required for each configuration along with the total estimated weight of the propeller. The estimated weight is taken from appendix C.

The propeller efficiency for the design cruise conditions for each propeller was estimated by the method given in the appendix of reference A-3. The efficiencies for best rate of climb, taken as 140 knots, and the static thrust were obtained with the aid of references A-3, A-4, and A-5.

The propeller noise levels for all configurations were estimated for a distance of 1,000 feet from the source by the method given in reference A-1 and are presented in table A-II. The noise levels in the table were calculated for a low power cruise condition (326 hp at 1,200 propeller rpm for the basic

engine-propeller gearing). The cruise velocity of the OV-1 airplane at sea level is approximately 140 knots for the 326 hp selected for this condition.

An examination of the data in table A-I and table A-II indicates it is possible to design markedly quieter propellers than the propeller installed on the OV-1 airplane with no loss in cruise performance. The results indicate the penalty in performance is about 1 percent in efficiency at best rate of climb (140 knots) and the penalty in static thrust is about 10 percent for an estimated reduction in noise level of 25 decibels.

REFERENCE

A-1. Hubbard, Harvey H.: Propeller Noise Charts for Transport Airplanes. NACA TN 2968, 1953.

A-2. Hubbard, Harvey H.; and Regier, Authur A.: Propeller-Loudness Charts for Light Airplanes. NACA TN 1358, 1947.

A-3. Crigler, John L.; and Jaquis, Robert E.: Propeller-Efficiency Charts for Light Airplanes. NACA TN 1338, 1947.

A-4. Crigler, John L.: Comparison of Calculated and Experimental Characteristics for Four, Six, and Eight Blade Single Rotating Propellers. NACA ACR No. 4F04, 1944.

A-5. Biermann, David; and Hartman, Edwin P.: Wind-Tunnel Tests of Four- and Six-Blade Single and Dual Rotating Tractor Propellers. Report No. 747, NACA, 1942.

TABLE A-I.- SUMMARY OF PERFORMANCE CALCULATIONS FOR PROPELLER CONFIGURATIONS

Variable Pitch - Constant Speed Propellers

Configuration	N, rpm	D	πnD	M_t	B	$\sigma_{.7R}$	η at 259 kts 1015 hp	η at 140 kts 960 hp	Static 960 hp	Weight, lb
Basic	1700	10	890	0.798	3	0.0381 B	0.860	0.820	3175	263.8
Modification I	1700	9	801	.718	5	.0343 B	.860	.810	3000	252.7
Modification II	1275	10	668	.598	5	.0381 B	.855	.810	2890	309.4
Modification III	1190	10	623	.558	6	.0343 B	.860	.810	2825	276.9

TABLE A-II.- SUMMARY OF SOUND PRESSURE LEVELS FOR PROPELLER CONFIGURATIONS

Propeller Configurations

Basic D=10.0 RPM=1200				Modification I D=9.0 RPM=1200			Modification II D=10.0 RPM=900			Modification III D=10.0 RPM=840		
f, cps	mB	dB calc	dB meas.	f, cps	mB	dB calc	f, cps	mB	dB calc	f, cps	mB	dB calc
60	3	90.5	90.0	100	5	81.0	75	5	74.0	84	6	65.0
120	6	79.5	84.0	200	10	56.5	150	10	42.0	168	12	
180	9	67.0	76.0									
240	12	54.5	76.0									
300	15		78.0									

APPENDIX B

WEIGHT ESTIMATES

M. L. Sisson

Propeller Weight Estimation

Propeller blade weights, for the standard rpm cases, are based on scaling factors applied to the existing Hamilton Standard blade. This method considers that the thickness-to-chord ratio at each percentage of propeller tip radius is maintained. The weight of the aluminum alloy blade becomes:

$$W_1 = \left(\frac{\text{chord}_1}{\text{chord}_0}\right)^2 \times \frac{\text{diameter}_1}{\text{diameter}_0} \times \text{weight}_0 ,$$

where subscript "0" refers to the original blade and subscript "1" refers to the new blade. A revised thickness distribution curve (figure B-1) was applied to the lower rpm cases (.75 and .70 times standard rpm). These blades were then scaled as above.

Propeller hub weights were scaled from the existing hub using a scaling factor which is the total blade centrifugal force (centrifugal force per blade times the number of blades) raised to the eight-tenths power.

Reduction gear weights were estimated by the Hamilton Standard equation, (reference B-1), $W = .095Q^{.84}$, for turbo-prop reduction gears. "W" is the reduction gear weight and "Q" is the output torque in pound feet.

REFERENCE

B-1 PDB6101 Supplement A, Hamilton Standard Propeller Weight Generalization, January 2, 1963; Hamilton Standard Division, United Aircraft Corporation.

Table B-I

Weight Estimates Per Propeller Installation

Production 3 blade, 10 foot diameter propeller

Hub plus blades	263.8 lbs.
Governor	64.9
Oil supply	14.8
One blade	47.3
Hub weight = $263.8 - 3 \times 47.3$	121.9
Gear (using Hamilton Standard equation, $W = .0959^{.84}$)	76

Modification 1
5 blade, 9 foot diameter, standard gear ratio

Blade weight = 5 x 28.5	142.5 lbs.
Hub weight	110.2
Total propeller weight	252.7 lbs.
Weight increase 252.7 - 263.8	-11.1 lbs.

Modification 2
5 blade, 10 foot diameter, gear ratio .75 x standard

Blade weight = 5 x 30.37	151.4 lbs.
Hub weight = .903 x 121.9	110.0
Total propeller weight	309.4 lbs.
Less original propeller	263.8
Propeller weight increase	45.6 lbs.
Gear weight increase = 95 - 76	19.0
Total weight increase	64.6 lbs.

Modification 3
6 blade, 10 foot diameter, gear ratio .7 x standard

Blade weight = 6 x 30.2	181.2 lbs.
Hub weight = .786 x 121.9	95.7
Total propeller weight	276.9 lbs.
Less original propeller	263.8
Propeller weight increase	13.1 lbs.
Gear weight increase = 104 - 76	28.0
Total weight increase per propeller	41.1 lbs.

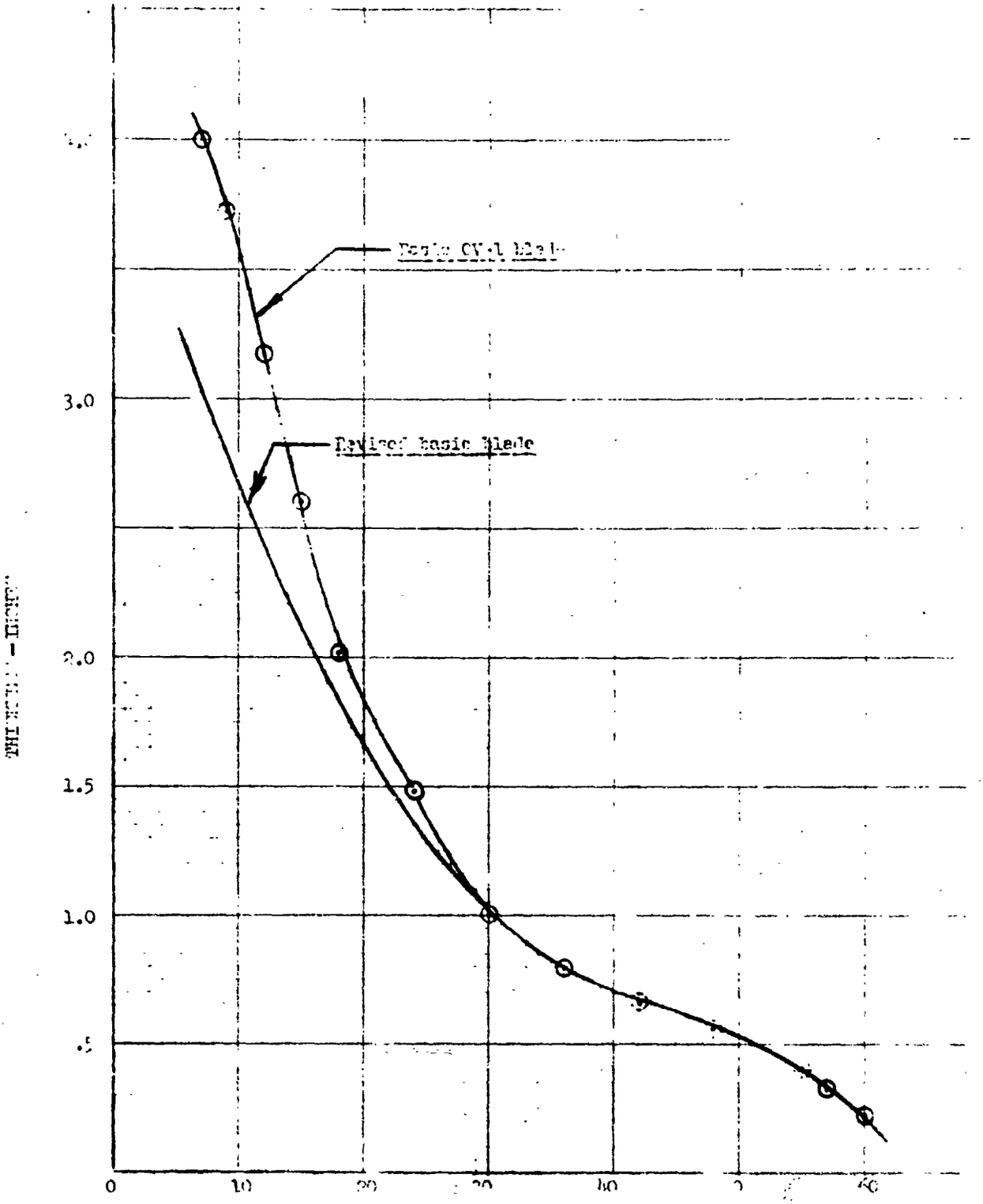

Propeller Blade Thickness Distribution

Figure . 1

APPENDIX C

PERFORMANCE, STABILITY, AND CONTROL

By James L. Hassell, Jr.

Method of estimating performance.- The thrust horsepower required for level flight for the basic OV-1A airplane cruise configuration was established by using the wind-tunnel lift-drag data of reference C-1 modified to agree with flight-test results given in reference C-2. Power required was calculated for a basic take-off gross weight of 12,148 pounds which corresponds to the Tactical Air Observation loading condition specified in reference C-3. Power required was also calculated for the various take-off gross weights of the modified configurations, using the same basic lift-drag polar. Thrust horsepower available for the basic OV-1A airplane was determined using the Lycoming T-53-L-3 turboprop engine data given in reference C-4 in conjunction with three-blade propeller characteristics of the Hamilton Standard Model 53C51 constant speed propeller. Thrust horsepower available for the various modified configurations with five- and six-bladed propellers was calculated using propeller characteristics derived from data of reference C-5. Flight performance was calculated by the classical methods utilizing the established power required-power available data. Static thrust and the variation of thrust with speed was calculated using as a basis the propeller thrust coefficients determined from reference C-5; these thrust characteristics were used for calculating the take-off distance to clear a 50-foot obstacle from a firm sod runway.

Basis for estimating changes in stability and control.- The only differences in stability and control characteristics from those of the basic

OV-1A airplane which might be anticipated would be associated with center-of-gravity shift due to changes in weight of the various propeller modifications and the effect of modified propeller slipstream on the horizontal and vertical tail surfaces. Neither of these effects were anticipated to cause changes of any real significance; however, check calculations were made to determine the probable extremes.

Results of performance calculations.- Performance calculations were made for the basic OV-1A airplane and for several modifications involving different propellers and reduction gearing. The take-off and landing gross weights associated with the basic and modified configurations are summarized in table C-I for the Tactical Air Observation loading condition. These weights were used in conjunction with the lift-drag polar presented in figure C-1 for calculating the thrust horsepower required for each configuration. The propeller characteristics for the basic and modified constant-speed propellers are presented in figure C-2 for sea-level military power conditions. These results were used in conjunction with the T-53-L-5 turboprop engine data to obtain thrust horsepower available for each configuration; 5 percent power losses were assumed in all calculations to account for compressor inlet and diffuser outlet duct losses, accessory power extraction, and other nonoptimum operating conditions. The thrust horsepower required and the two-engine power-available results are presented in figures C-3 and C-4 for the sea-level take-off power, military power, and normal rated power conditions. The variation of thrust with velocity was calculated for the sea level take-off power condition for each configuration and is presented in figure C-5.

The flight performance of the basic and modified configurations was calculated using the power available - power required data as a basis, and

the take-off performance was calculated using the thrust as a function of velocity as a basis. These calculated results are summarized in table C-II. A cursory study of this table indicates that of the various performance items tabulated, only the take-off distance to clear a 50-foot obstacle and the maximum rate-of-climb capability suffer to any extent as a result of the various modifications. The least acceptable calculated performance was obtained with modification II for which the take-off distance to clear a 50-foot obstacle was 8.6 percent longer and the maximum rate-of-climb at sea-level was 3.8 percent less than the basic OV-1A. The main reason for the reduced performance of the modified configurations in take-off and climb is the lower static thrust (fig. C-5) and the slightly lower propeller efficiencies at the speeds for best rate of climb (fig. C-2). It should be noted that stall speed and maximum speed are relatively unaffected by the various modifications despite some moderate weight increases for modifications II and III. The reasons for this result is that the aerodynamic characteristics of the OV-1A were unaffected by the various modifications and the propeller efficiencies at high speed were almost equal to that of the basic OV-1A propeller.

Results of stability and control study.- As indicated by the results of weight and balance calculations presented in table C-I, the various modifications had relatively little effect on the center-of-gravity location of the aircraft. In general, increased propeller weight tended to move the center of gravity forward slightly. The heaviest installation (mod. II) resulted in a forward shift of less than 1 percent mean aerodynamic chord. Therefore, the static longitudinal stability of the aircraft would be improved

in direct relationship to this forward center-of-gravity shift. The most forward center-of-gravity position is within the design forward limit for the OV-1A airplane.

A brief analysis was made of the dynamic pressure in the region of the aircraft empennage as affected by propeller slipstream for velocities up to 120 knots. The dynamic pressure at the tail was calculated from the expression:

$$q_t = q_o + \frac{4T}{\pi D^2}$$

where:

q_t = dynamic pressure at the tail

q_o = free-stream dynamic pressure

$$\frac{4T}{\pi D^2} = \frac{T}{A} = \frac{\text{thrust}}{\text{propeller disk area}}$$

The results of these calculations for the basic OV-1A and the modified configurations are presented in figure C-6. These calculations indicate that the 9-foot-diameter propeller (mod. I) would produce increases in q_t ranging from 7.7 to 16 percent whereas the 10-foot-diameter propellers (mods. II and III) would result in decreases in q_t ranging from 0.7 to 10.5 percent. What this means in terms of aircraft handling qualities is that the response to elevator and rudder control at a given speed would be more sensitive in the case of the 9-foot-diameter propellers and less sensitive in the case of the 10-foot-diameter propellers, and the change in sensitivity would be directly proportional to the change in dynamic pressure at the tail. These propeller slipstream effects have no bearing on the tail contributions to either longitudinal or lateral directional stability, of course.

REFERENCES

C-1. Shepheard, F. W.: Wind-Tunnel Tests of 1/7-Scale Model OV-1. USAAVLABS Technical Report 65-73, December 1965.

C-2. Ramsey, Paul H.: Combined Stability and Control and Aircraft and Engine Performance Trails of the AO-1CF Airplane. Report No. 1, Final Report, Project No. BlS 21246, September 1962.

C-3. Anon: Model AO-1AF Contract NOw 60-0040-r, Grumman Aircraft Engineering Corp. Report 395lJ, April 10, 1961.

C-4. Anon: T53-L-3 Turboprop Engine (Lycoming Model LTC1F-1). Specification No. 104.11-C, Lycoming Division of AVCO Corp., March 25, 1961.

C-5. Biermann, David; and Hartman, Edwin P.: Wind-Tunnel Tests of Four- and Six-Blade Single- and Dual-Rotating Tractor Propellers. NACA TR 747, 1942.

TABLE C-I.- WEIGHT AND BALANCE SUMMARY

Case	Condition	Weight empty, lb	Gross weight, lb	Gross weight, c.g., % MAC
Basic	Take-off	9564.8	12,148.1	26.6
	Landing		11,043.0	26.6
Mod. I	Take-off	9542.6	12,125.9	26.7
	Landing		11,020.8	26.7
Mod. II	Take-off	9675.0	12,277.3	26.1
	Landing		11,172.2	26.0
Mod. III	Take-off	9647.0	12,230.3	26.2
	Landing		11,125.2	26.1

Note: Useful load for all cases assumed fixed and is defined in the mission summary of reference C-3, page 6.01. Total useful load is 2583.3 pounds and includes 1842 pounds fuel at take-off. Landing condition assumes 40 percent fuel load.

TABLE C-II.- PERFORMANCE SUMMARY

Item		Basic OV-1A	Modification I	Modification II	Modification III
Gross weight, lb		12,148.1	12,125.9	12,277.3	12,230.3
Propeller blades		3	5	5	6
Propeller diameter, ft		10	9	10	10
Gear reduction		Basic	Basic	.75:1	.70:1
Take-off distance at SL with T.O. rated power:					
Ground run, ft		723	765	810	793
Air distance to clear 50-foot obstacle, ft		350	351	355	353
Total T.O. distance, ft		1,073	1,116	1,165	1,146
Percent more than basic		-----	4.0	8.6	6.8
Maximum rate of climb with NRP, ft per min	SL	2,416	2,383	2,325	2,328
	5,000	2,101	2,066	2,017	2,018
	10,000	1,748	1,713	1,668	1,671
	15,000	1,410	1,383	1,335	1,342
	20,000	995	976	935	943
	25,000	511	507	464	467
NRP service ceiling		29,300	29,300	28,800	28,800
Velocity for best rate of climb with NRP, knots, TAS	SL	139	139	139	139
	5,000	139	139	140	140
	10,000	144	144	145	145
	15,000	144	144	144	144
	20,000	156	156	157	157
	25,000	170	170	171	171

TABLE C-II.- PERFORMANCE SUMMARY - Continued

Item		Basic OV-1A	Modification I	Modification II	Modification III
V_{max} with NRP, knots, TAS	SL	242	242	241	241
	5,000	245	245	244	244
	10,000	249	249	248	248
	15,000	248	248	247	246
	20,000	245	245	244	244
	25,000	231	232	230	230
Maximum rate of climb with MRP, ft per min	SL	2,805	2,768	2,703	2,710
	5,000	2,431	2,389	2,339	2,341
	10,000	2,015	1,977	1,929	1,940
	15,000	1,622	1,593	1,543	1,551
	20,000	1,146	1,124	1,082	1,094
	25,000	640	636	592	596
MRP service ceiling		30,000	30,000	29,600	29,600
Velocity for best rate of climb with MRP, knots, TAS	SL	139	139	139	139
	5,000	139	139	139	139
	10,000	144	144	145	145
	15,000	144	144	144	144
	20,000	156	156	157	157
	25,000	170	170	171	171
V_{max} with MRP, knots, TAS	SL	252	252	251	251
	5,000	254	254	255	254
	10,000	256	256	255	355
	15,000	256	256	255	256
	20,000	252	252	251	252
	25,000	241	241	239	238

TABLE C-II.- PERFORMANCE SUMMARY - Concluded

Item		Basic OV-1A	Modification		
			I	II	III
Cruise configuration V_{stall}, knots, TAS	SL	94	94	94	94
	5,000	101	101	102	102
	10,000	109	109	110	110
	15,000	119	118	119	119
	20,000	129	129	129	129
	25,000	140	140	141	141

Note: Five percent power losses were assumed in all performance calculations to account for duct losses, accessory power extraction, and other nonoptimum operating conditions.

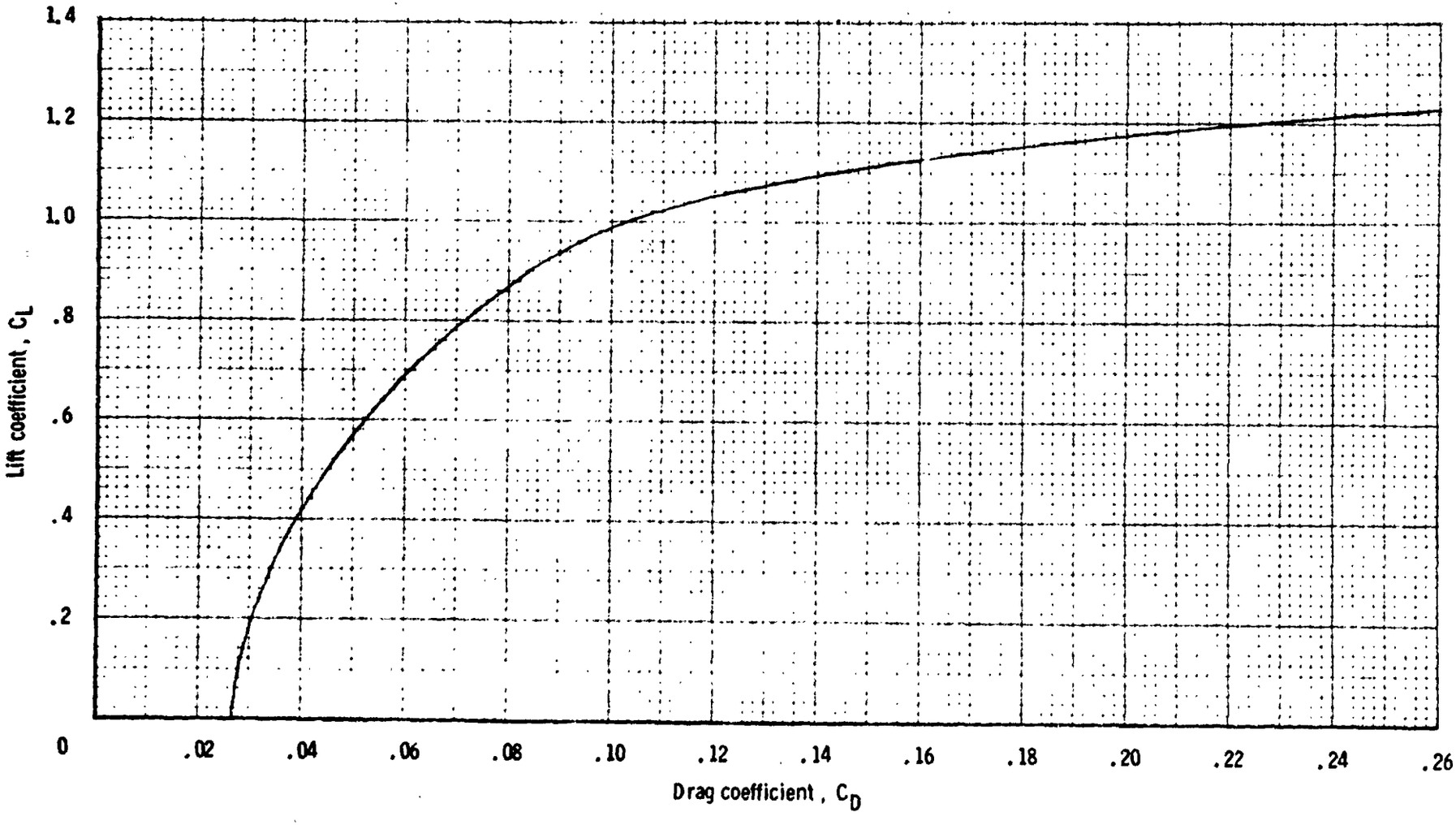

Figure C-1.- Lift - drag polar for the basic OV-1A airplane, cruise configuration (from reference C-1 modified to match full-scale flight test results of reference C-2).

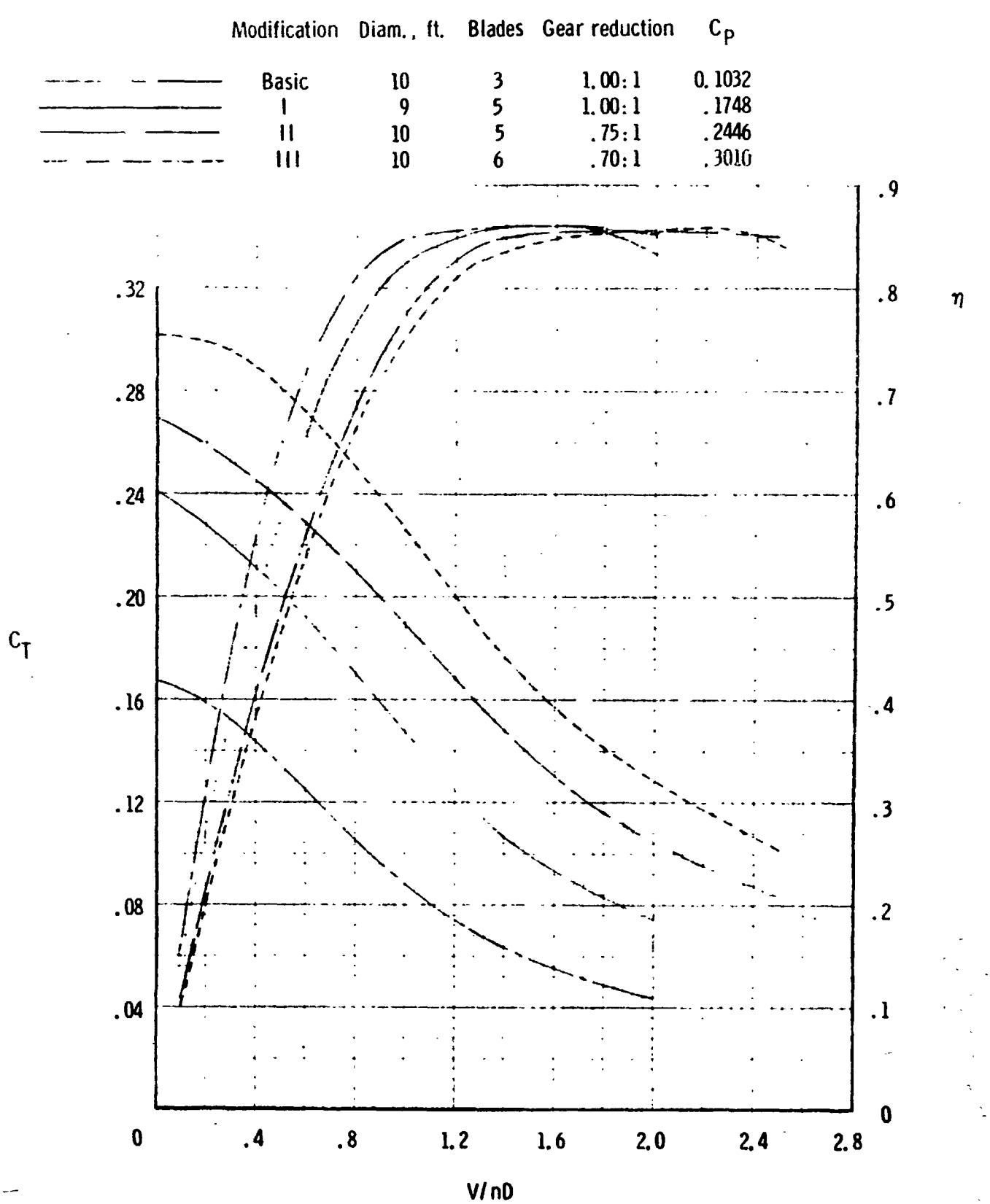

Figure C-2. - Thrust coefficient and efficiency curves for the basic and modified constant-speed propellers at sea level, military rated power of the T-53-L-3 engine.

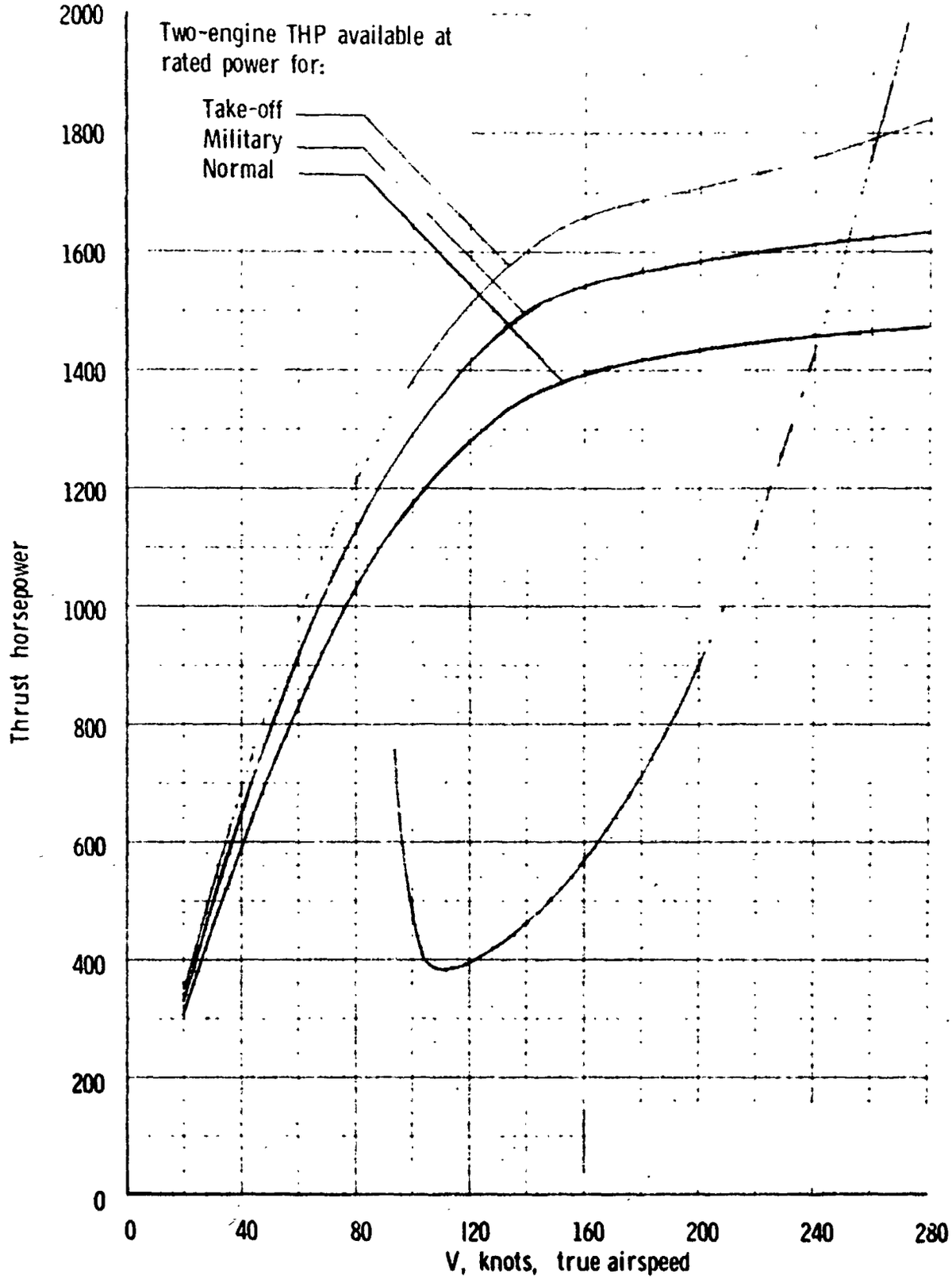

Figure C-3. - Power available and power required for the basic OV-1A airplane, cruise configuration, at sea level standard conditions.

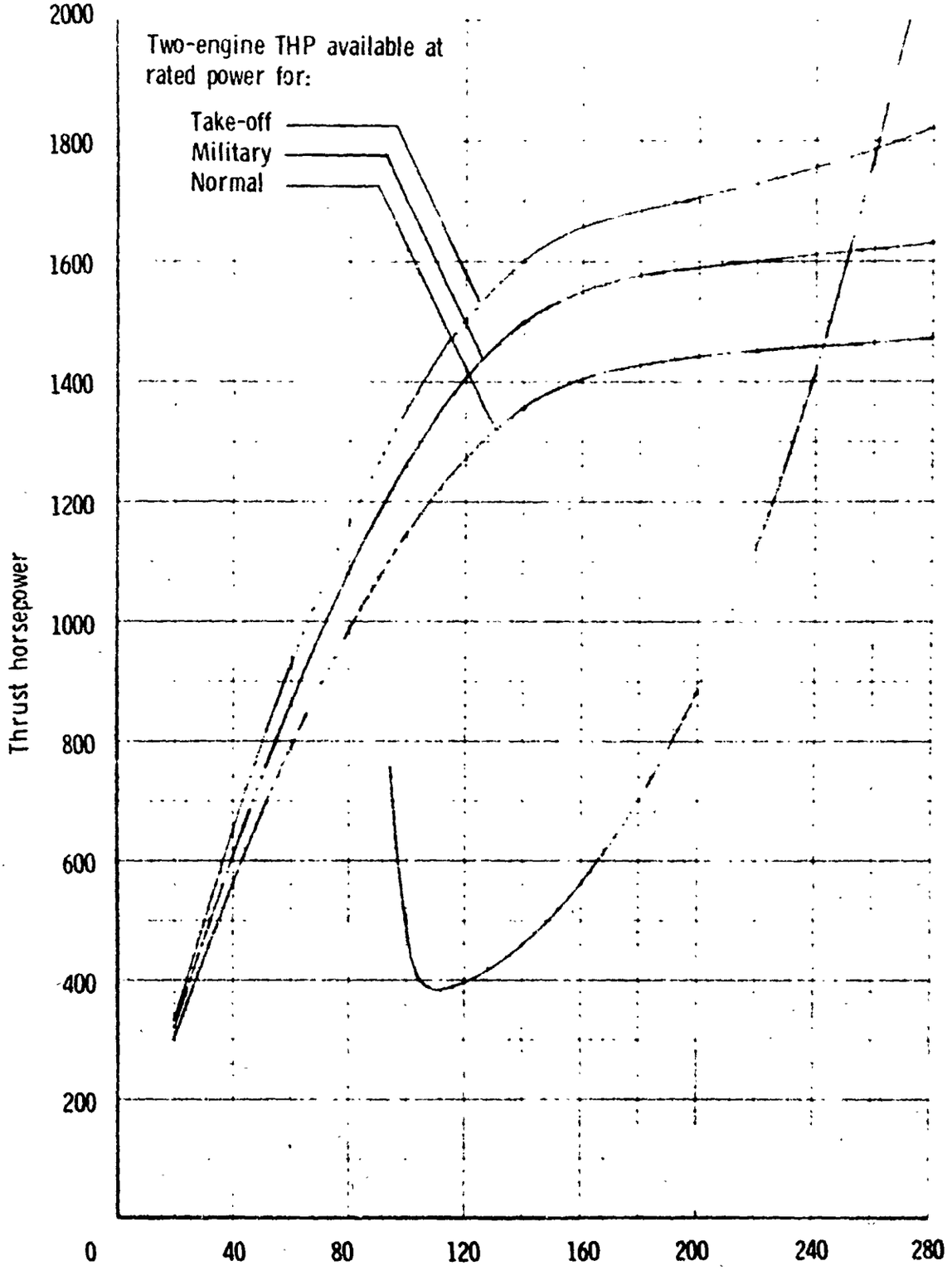

(a) Modification I (D = 9 ft., 5 blades, gear ratio 1.00:1, 1700 rpm).

Figure C-4. - Power available and power required for modified configurations.

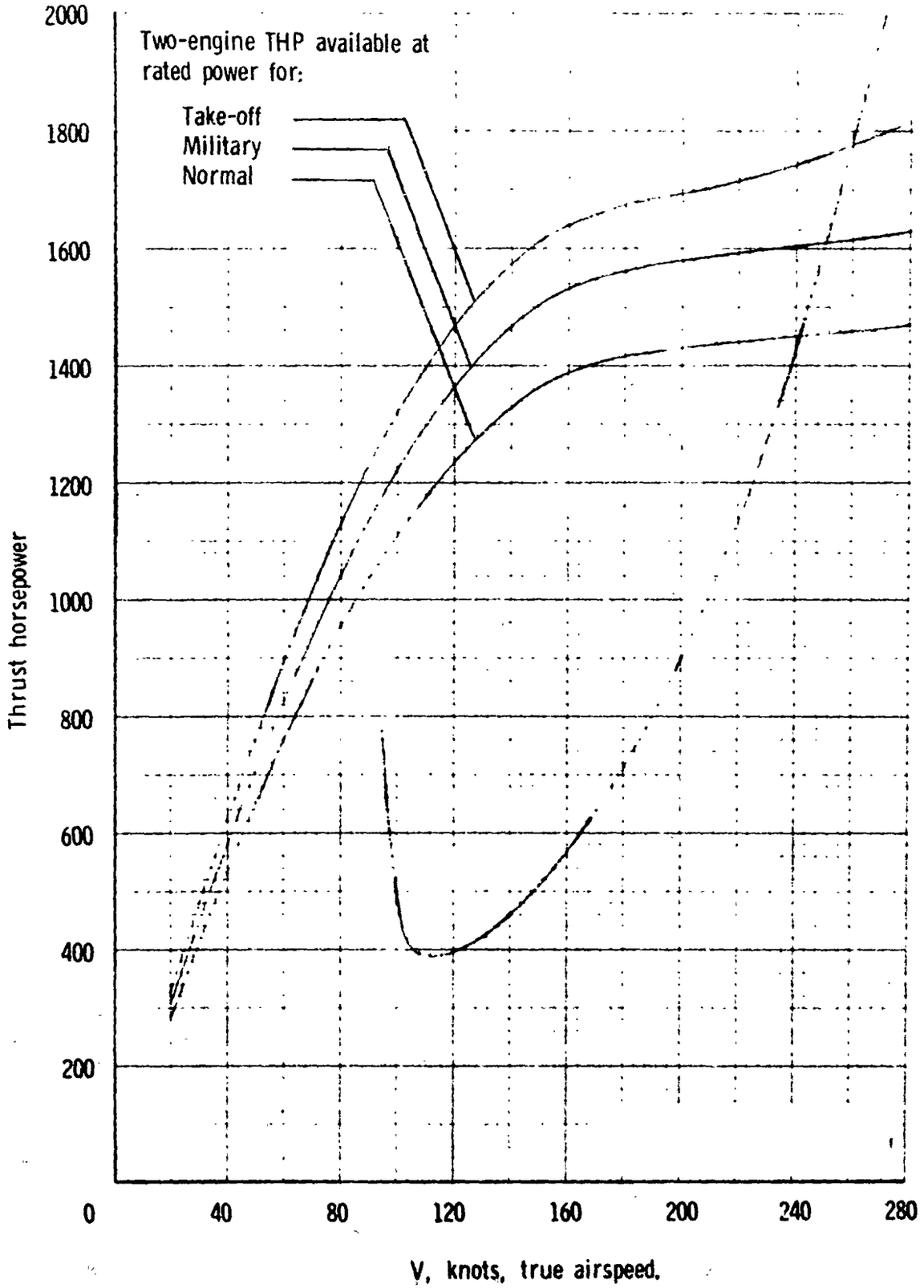

(b) Modification 11 (D = 10 ft., 5 blades, gear ratio 0.75:1, 1275 rpm).

Figure C-4. - Continued.

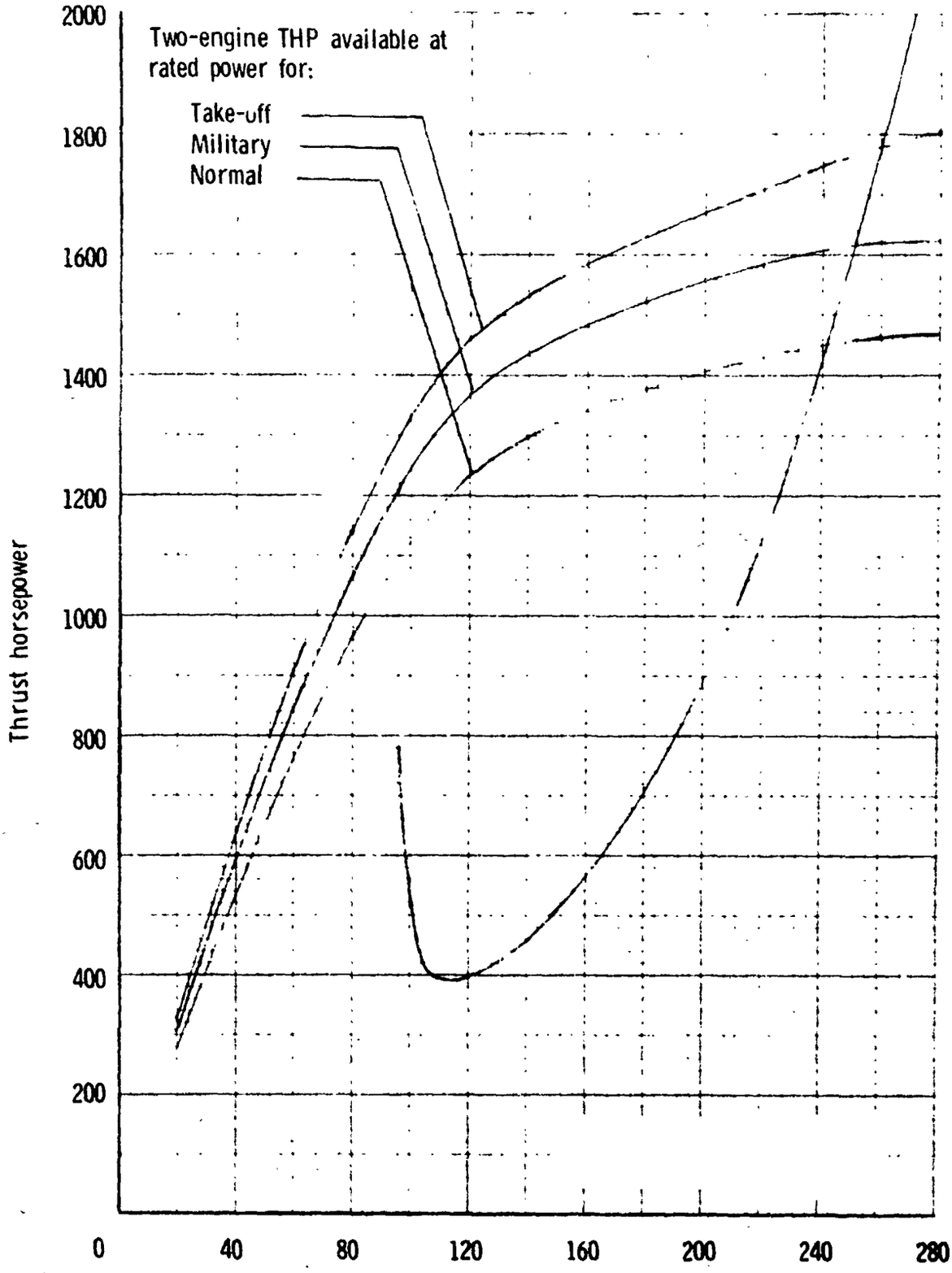

(c) Modification III (D = 10 ft., 6 blades, gear ratio 0.70:1, 1190 rpm).

Figure C-4. - Concluded.

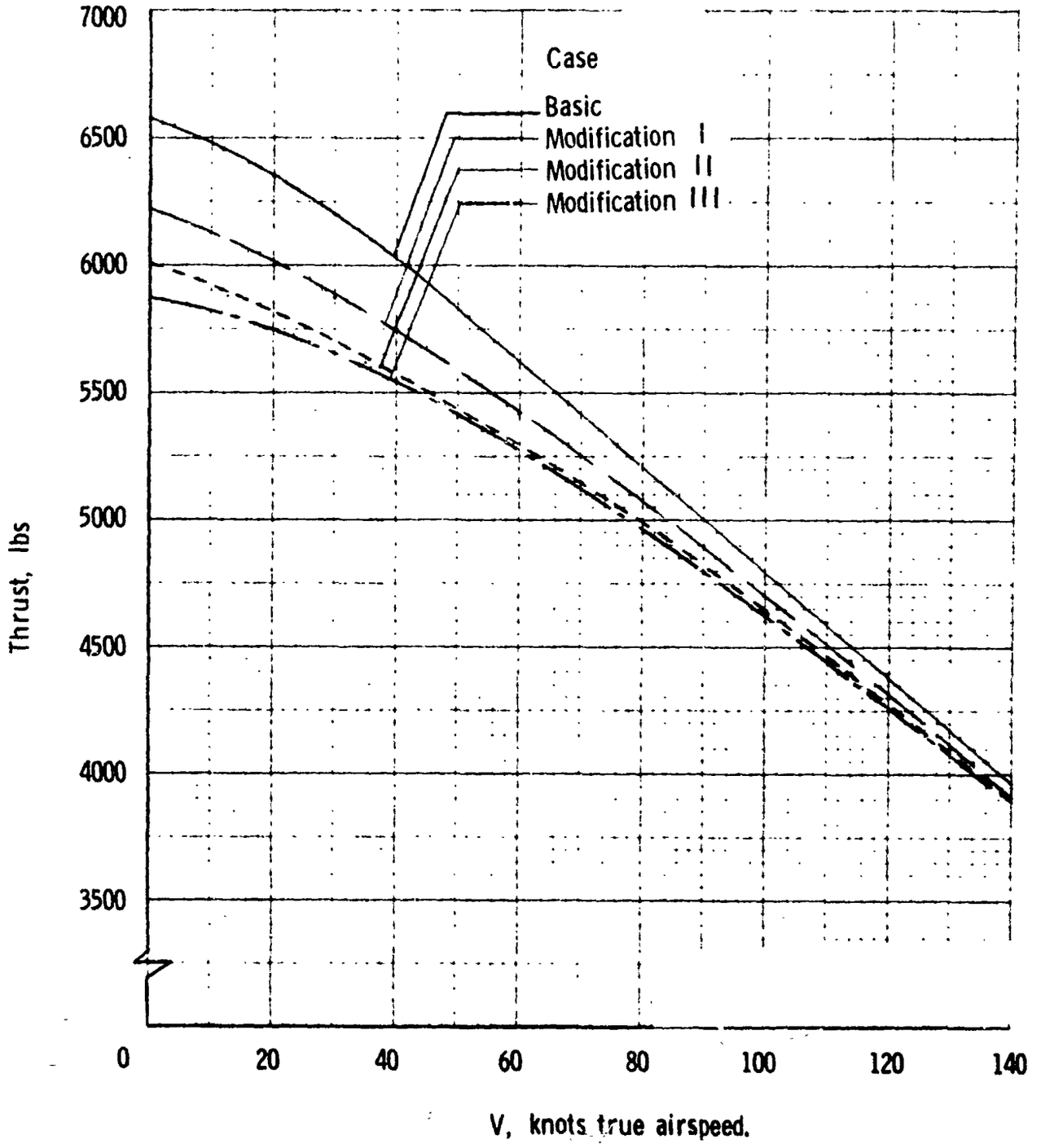

Figure C-5. - Variation of thrust with velocity with two-engine take-off rated power at sea level standard conditions. (Data includes residual jet thrust.)

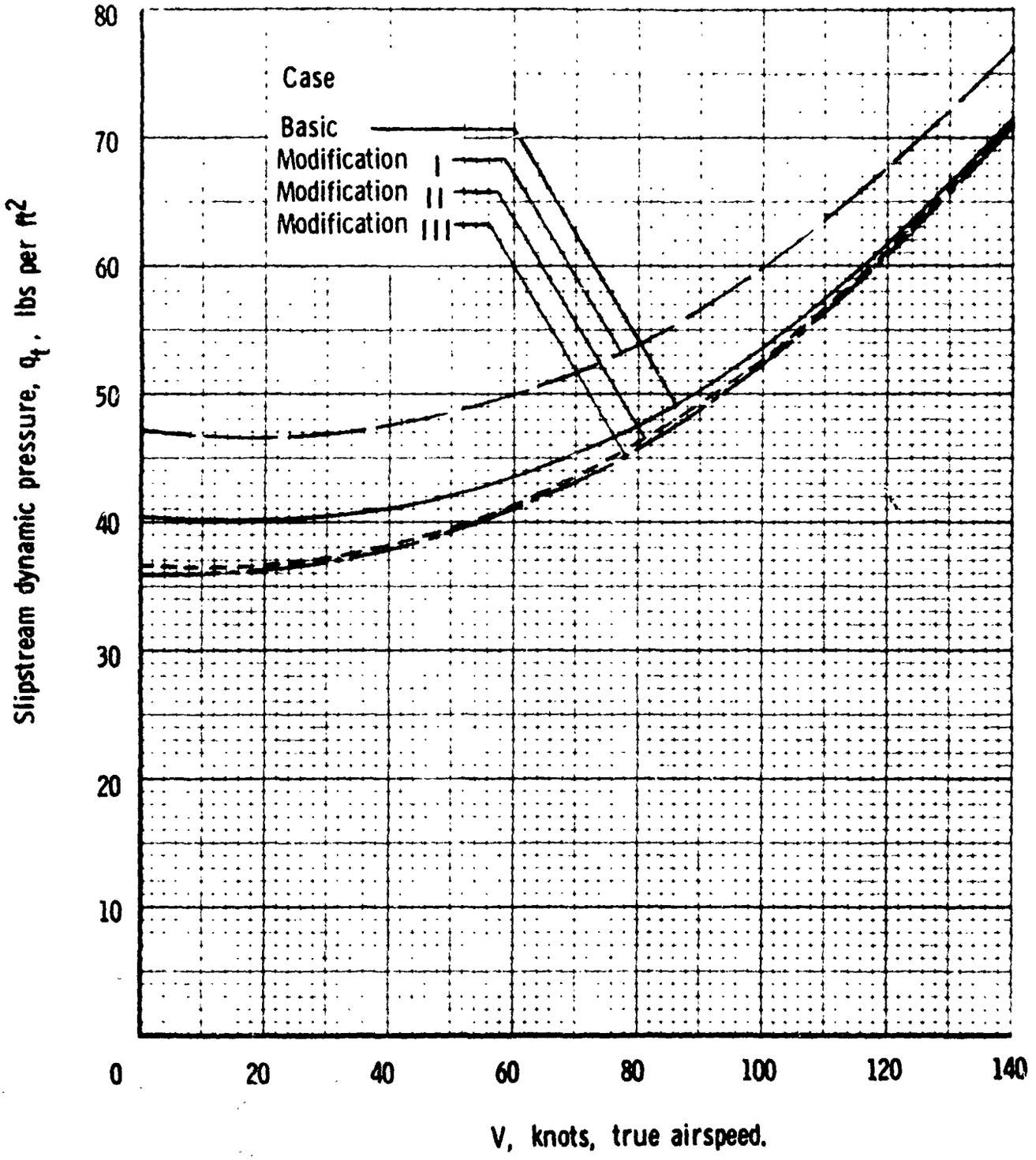

Figure C-6. - Calculated variation of slipstream dynamic pressure with airspeed for take-off rated power.